Title
THRESHOLD DETECTOR APPLICATIONS TO NEUTRON SPECTROSCOPY AT THE BERKELEY ACCELERATORS

Author
Smith, Alan R.

Publication Date
1965-11-19

UCRL-16312

University of California

Ernest O. Lawrence Radiation Laboratory

THRESHOLD DETECTOR APPLICATIONS TO
NEUTRON SPECTROSCOPY AT THE BERKELEY ACCELERATORS

Berkeley, California

DISCLAIMER

UCRL-16312

UNIVERSITY OF CALIFORNIA

Lawrence Radiation Laboratory
Berkeley, California

AEC Contract No. W-7405-eng-48

THRESHOLD DETECTOR APPLICATIONS TO NEUTRON SPECTROSCOPY AT THE BERKELEY ACCELERATORS

Alan R. Smith

November 19, 1965

THRESHOLD DETECTOR APPLICATIONS TO NEUTRON SPECTROSCOPY AT THE BERKELEY ACCELERATORS*

Alan R. Smith

Lawrence Radiation Laboratory
University of California
Berkeley, California

November 19, 1965

ABSTRACT

The nuclear physicist's technique of studying nuclear reactions by bombardment of target elements with known-energy neutrons can, in a sense, be inverted to permit study of unknown-energy neutrons by observation of known reactions in bombarded target elements. A selected group of these reactions, with well-known excitation functions of dissimilar energy thresholds, can be used to measure the incident-neutron energy spectrum. We can divide threshold detectors into two types: prompt detectors (pulse counters), which report information while in the radiation field; and, passive detectors (activation elements), which are examined for information content after removal from the radiation field.

Although such detectors have often been used for neutron spectroscopy in high fluxes of fission-produced neutrons, their application in accelerator-produced neutron fields has been very limited--particularly where low (occupational) flux intensities are encountered. We have made considerable progress in adapting threshold detectors for particle accelerator applications, and have extended the useful energy range upwards while also improving sensitivity to accommodate low-flux situations. Two systems of these detectors are now in operation at Berkeley; we describe the systems, cite examples of their use, and discuss some important unsolved problems related to our applications of the detectors.

The first system consists of activation elements only, and provides neutron spectral information over the energy range 2 to 30 MeV. Among the activation elements are aluminum, carbon, cobalt, copper, iodine, iron, magnesium, nickel, and titanium. Induced activities are observed by γ-ray scintillation spectrometry, the only reasonable analysis method that permits extension of this technique to low intensities of neutron flux. Digital computer programs are used for γ-ray spectral

---

*For the First Symposium on Accelerator Radiation Dosimetry and Experience, Brookhaven National Laboratory, November 3-5, 1965. To be presented at SESSION II.

analysis, and are also used in calculation of the neutron spectra we seek to determine. Some results obtained at the Bevatron are discussed, in terms of the spectra themselves, and in terms of the unsolved problems attendant on this technique. Among these problems are complexities of γ-ray spectra, lack of neutron cross-section data at energies higher than about 15 MeV, and production of desired activities by particles other than neutrons.

The second threshold detector set consists of a mixed system of both pulse counters and activation elements, including moderated foil or BF_3 counter, aluminum disc, carbon (in the form of plastic scintillator), and bismuth fission counter. Detector information is related to the neutron spectrum over an energy range extending from about 0.02 MeV up to the primary particle energy. Data analysis involves use of a simple digital computer program, which incorporates detector calibrations, reaction cross sections, and trial neutron spectra as input parameters. The objective of this program is to compute a detector response that matches the observed detector response; attainment of this goal defines the neutron spectrum "measured" by our detectors. The effects of reasonable variations of input parameters on calculated detector response are described, and an example of a neutron spectrum that fits data obtained at the Bevatron is discussed.

At present the mixed system of threshold detectors can supply only the broad general shape of a neutron spectrum, but can encompass the entire energy range produced by the source; furthermore, exposure of detectors, counting, and data anlaysis can be completed in a few hours. In contrast, the activation-element set can provide considerable detail over a limited neutron energy range, and requires lengthy data-analysis time. Both methods could be greatly improved if all the required cross-section data were known.

I. INTRODUCTION

Our subject concerns the use of threshold detectors for neutron spectroscopy, with particular emphasis on application of these detectors to Health Physics problems. In this context, we must often measure weak neutron fields where flux intensities are less than 100 n/cm^2-sec; furthermore, the flux may be so nearly isotropic that neutron spectrometers that use incident particle direction as a measurement parameter cannot be profitably employed. Thus we must rely on high-sensitivity 4π spectrometer systems to provide information in such situations.

We discuss two of these systems here. The first system consists of activation elements only. Formalism for our version of this method was originally developed by Ringle,[1] and was later modified by Kohler.[2] Ringle and Wadman[3] have applied the method to detectors irradiated inside the shield near targets at the 88-inch cyclotron. Kohler has applied the modified formalism to data acquired from a shield array experiment at the 6.2-BeV Bevatron. The second system consists both of activation elements and of prompt counters. It has been used at the Bevatron and the 184-inch cyclotron to provide information on neutron spectra at locations outside the accelerator shields.

The material presented here is closely related to topics discussed in another paper to be given later at this symposium,[4] a paper that deals with shielding measurements taken at the Bevatron. Similar or identical techniques have been employed in experimental efforts that comprise the basis for both presentations. Some duplication of material in the two papers seems unavoidable, in the interests of clarity and continuity of exposition. Considerable thought has been given this problem, and we hope that such repetition has been held to an acceptable minimum.

II. GENERAL CONSIDERATIONS

Threshold detectors can be considered to belong to either of two categories: prompt counters, which report information while in the radiation field; and activation elements, which are examined for induced radioactivity after removal from the radiation field.

Prompt counters are the more sensitive of the two on the basis of observed events per gram of active material. However, this high intrinsic sensitivity cannot always be utilized, because we may not be able to incorporate a large amount of the active material into a counter. There may be difficulty in distinguishing the desired class of events in the presence of unwanted events; there may also be a problem of count loss due to high instantaneous flux intensity. Additional factors that may become problems include accessibility to exposure sites, reliability

of counters and associated electronics, and the number of sites to be studied simultaneously.

The intent of our discussion here is not to discourage the use of prompt counters, but is just to indicate that there are a number of problems associated with their use. These problems can often be solved satisfactorily; furthermore, prompt counters possess the distinct advantage of providing information concurrent with the exposure. We do point out that such problems constitute some of the major reasons for use of activation-element threshold detectors.

Activation elements are relatively insensitive on the basis of observed events per gram of active material; however, we can often compensate for this low intrinsic sensitivity by using large amounts of material--kilograms, for example. These elements are immune to problems posed by high instantaneous flux intensities; they are also easily put into cramped quarters or limited space, and there is no problem of "reliability" for an element during exposure. The number of sites that can be studied at one time is limited only by the amount of decay of observed radioisotopes that can be tolerated during subsequent activity-analysis periods.

The primary analysis tool for activation elements is the NaI(Tl) scintillation crystal γ-ray spectrometer. Gamma-ray spectra thus acquired may be quite complex, and we often encounter problems in distinguishing desired activities from unwanted activities in such spectra. A discussion of these problems, along with some suggested solutions, can be found in a later section of our presentation. We note that information from activation elements is available only after an exposure, in contrast to the concurrent data furnished by prompt counters; activation elements are clearly at a disadvantage in this context.

We see that each type of detector has advantages and disadvantages in comparison with the other. Choice of a detector array may also be influenced by practical circumstances, so the resultant choice is usually a compromise among a number of factors. For the first system we describe, the requirements of restricted space and simultaneous measurements are particularly important. For the second system, the property of very high sensitivity is a dominant factor in detector selection.

When fast neutrons of various energies bombard selected target elements, a number of nuclear reactions may be possible. For each reaction, there is an energy for incident neutrons below which the reaction cannot occur; for every energy value above this threshold point, the reaction can be characterized by a single value for the cross section, or probability of occurrence. These characteristics of nuclear reactions--the existence of an energy threshold, and the single-valued nature of the cross-section function--can be used as the basis for a system to measure neutron energy spectra.

We employ a number of nuclear reactions, which have different neutron-energy thresholds and dissimilar cross section shapes above the threshold energy. For each reaction, there exists the following relationship among detector activity, cross section, and neutron flux:

$$A_i' = \int_0^\infty \phi(E)\ \sigma_i(E)\ dE, \qquad (1)$$

where A_i' = detector saturation activity or disintegration rate per target nucleus in sec^{-1},

$\phi(E)$ = neutron flux in $cm^{-2}\ sec^{-1}\ MeV^{-1}$,

$\sigma(E)$ = reaction cross section in cm^2,

E = neutron energy in MeV,

i = subscript identifying the reaction and residual nucleus.

A set of these equations can, in favorable circumstances, be solved for the unknown flux and spectrum. Equation 1 is called a Fredholm equation of the first kind, and its solution is quite difficult in many cases. Discussion of solutions can be found in Morse and Feshbach;[5] examples of solution methods applied to our particular problem can be found in Ringle's report.

III. ACTIVATION-ELEMENT SYSTEM

A. Description of System

Our spectroscopy method was designed to cover the neutron energy range from 2 to 30 MeV. Neutron reactions of the types (n, p), (n, α), and (n, 2n) were selected, partly on the basis of the energy range to be investigated, and partly on the basis of available cross-section data. Criteria were established for selection of the threshold materials; these included physical, chemical, and economic factors, as well as nuclear properties. Economic factors are of considerable importance, because kilogram quantities of threshold elements may be required for successful determinations in area where flux intensities may be less than $\approx 100\ n/cm^2\text{-sec}$. Table 1 lists some reactions found to be useful in our studies. Table 2 lists some additional simple reactions that appear promising for future work; this list is by no means complete and could be greatly enlarged. However, cross-section values are not well known for many potentially useful reactions and we are presently limited in reaction choice by this problem.

We define useful threshold reactions to be those which produce radioisotopes whose decay is accompanied by γ-ray emission. Our samples are 4 in. in diameter and may be up to 1 in. thick; only by observing γ rays can we achieve high detection efficiency from such thick samples. Gamma-ray detection is accomplished with a scintillation crystal spectrometer system; the detector is a single 4-in.-diameter by 2-in.-thick NaI(Tl) crystal, and its output is presented on a 100-channel pulse-height analyzer (PHA). As a matter of course the spectrometer system is carefully maintained and kept in calibration. The equipment is in constant and purposeful use, and so is always capable of producing meaningful information. The NaI(Tl) crystal is used in a specially constructed low-background shield enclosure,[6] to facilitate assay of very small quantities of radioisotopes. The background count rate in the crystal is both very low and very constant--two conditions without which these small activities cannot be measured accurately.

B. Gamma-Ray Spectral Analysis Method

Analysis of γ-ray spectra is performed with a rather simple spectrum-stripping technique that requires a minimum of "library" or reference spectral shapes. To resolve a spectrum into its components, we start at the high-energy end and work toward the low-energy end--the usual direction for spectrum-stripping techniques. Each component is resolved singly, with the aid of a digital computer program that gives a solution for both the total absorption peak and its associated Compton distribution. The only library functions required are those from which Compton distributions are derived. The total absorption peak area is computed by a nonlinear least-squares technique that fits a Gaussian shape to actual data points. The quantity of radioisotope that produced the observed response is then computed from this value of peak area. The radioisotope quantity is the output of our γ-ray spectrum analysis program, and becomes the input for the neutron spectrum computation program.

Details of the γ-ray analysis program can be found in Ringle's report. We omit most of this detail here, but include several items that are particularly relevant to our experience with the method.

The method possesses two advantages that are quite important to our purpose. First, there is automatic compensation for small (but troublesome) changes in system gain. We tell the computer only the position of a peak, not its true energy; the computer calculates an energy that belongs with a peak at the specified position. It then uses this energy to generate a Compton distribution. Consider that the system gain has increased slightly relative to calibration conditions. A particular-energy peak will appear at a higher-than-normal position; the associated Compton edge will also move upscale, an almost equal amount. Here is just the compensation we would have to introduce in some fashion if

meaningful results are expected from "gain-shifted" spectra. More elegant schemes are often used for gain-shift correction; however, our method has proved satisfactory for the present situation, so we have not adopted a more sophisticated approach.

The second advantage is that we require only a small array of "library" or reference spectra; these are used to generate Compton distributions, not entire spectral shapes. A number of more elaborate (and potentially more precise) methods for analysis of complex γ-ray spectra have been developed. These were examined, and rejected on the following basis. Such schemes require extensive libraries of exact response functions: for example, a complete set of spectral shapes for every isotope likely to be encountered in a sample under investigation. If various shapes, sizes, or counting distances are used, it may be necessary to have complete sets of response functions for each combination of these variables.

We may wish to span a neutron flux intensity range of 10^6 in a simultaneous exposure of several detector sets, and the resulting activities may show a range of γ-ray emission rates in excess of 10^8, because of differences in reaction cross sections, half-lives, and decay schemes. We cannot handle such a wide range of activity in a fixed sample-detector relationship; thus the necessity to vary both sample size and counting distance. Generation of the required large number of exact response functions seemed so monumental a task that it was not given serious consideration. We sought a simpler method, and developed the scheme outlined above.

Our γ-ray analysis method was selected before we undertook the Bevatron shield array experiment. We are now reexamining the method in light of this experience, an experience that has clearly demonstrated some defects in the procedure. For example, considerable difficulty was encountered in selection of the correct value for a continuum that lies beneath the uppermost peak to be analyzed. (This continuum represents contributions from γ rays whose energies lie beyond the upper boundary of our observed spectral interval, and must be removed before computer analysis can proceed.) Furthermore, we assume the continuum to be a featureless distribution. This assumption is not always valid, and some errors may be thus introduced into analysis results. If spectra are very complex and contain overlapping peaks, the method does not work at all if the peak of interest occurs in this overlapping structure; similarly, the presence of an interfering peak directly beneath the peak of interest can cause serious errors in our results.

These difficulties in the γ-ray spectrum-analysis method have caused considerable extra work. We may have to do a series of graphical studies (by hand) to determine the proper value for the underlying continuum. We may be forced to take successive γ-ray spectra from

each sample during various stages of activity decay, so that we can obtain spectra in which the peaks of interest stand "in the clear." We illustrate the nature of these problems in Figs. 1 and 2, which show some γ-ray spectra observed with our normal energy scale, from 0.08 to 2.08 MeV.

The spectra on Fig. 1 are from an aluminum disc irradiated at the Bevatron. The upper curve shows only Na^{24}, the desired activity; the lower curve shows only Na^{22}, again the desired activity but observed at a later time. The Na^{22} curve was actually observed at much lower intensity than shown here, so it did not cause any interference with the Na^{24} curve. The Na^{24} curve is an example of a single radioisotope spectrum, in which we must subtract the continuum beneath the uppermost peak before analysis of this peak can be performed. Selection of a value for this continuum is seen to be a matter that may require some study.

The spectra on Fig. 2 are a repetitive series of analyses for a titanium disc irradiated at the Bevatron. The point we stress here is the interfering pattern caused by several γ rays whose energies are so closely spaced that the scintillation crystal cannot resolve the structure into separate peaks. We will refer to titanium and this spectral complexity again in a later section. For the moment, it is sufficient to comment that we wish to observe γ-ray peaks at energies of 0.89, 0.99—1.04, 1.12, 1.16, and 1.32 MeV; our analysis method cannot do this from any single spectrum shown here, and can perform the job only with considerable difficulty from the entire spectral set.

The Bevatron experiment provided a latitude that encompasses the entire range of detector activities we expect to encounter. We are studying this experience to determine whether it is possible to select a few values for detector size and counting distance, so that a more sophisticated γ-ray analysis method can be employed. Adoption of such a method would entail the generation of complete library spectra, and so limiting the counting "geometry" is vital to success.

C. Bevatron Shield Array Experiment

1. Description of Experiment

Our experiment concerns the shielding of high-energy particle accelerators. For this purpose, we use the 6-BeV external proton beam produced by the Bevatron. Figure 3 shows a plan view of the experimental setup. The primary proton beam enters from the right along a shielded channel; this channel narrows to a 2×2-ft cross-section area about 8 ft ahead of the shield array. A thin plastic scintillator is located at the front of the narrow channel and is viewed by closed-circuit television. The position and size of the beam spot are continuously observed in this fashion; correct beam alignment is verified by reference to a grid

scribed on the scintillator. The beam spot was usually no greater than 2 in. in extent as viewed by the scintillator-television system.

The shield array consists of ordinary concrete is block form, and is 28 ft thick along the beam line, 22 ft wide, and 18 ft high. Slots provide access to the beam line at 4-ft intervals. Several special thin blocks are seen at the front of the array, to allow more detailed study in this region; access is from the top for these positions. Rows of blocks are separated by 3-in.-wide gaps to allow insertion of detectors. All portions of these gaps, except the 18-in.-high slots actually used for detector placement, are filled with gypsum wallboard, to minimize air spaces along which neutrons could scatter or diffuse.

Figure 4, a photograph of the working face of the array, gives some idea of the actual setup and the manner in which it was used. A wooden trough, loaded with detectors, has just been inserted in one of the slots; all detectors were positioned for exposure in this fashion.

The principal detectors are the activation-threshold type. In such a detector, one observes an integrated response that can be produced only by neutrons (or protons) whose energy is greater than some "threshold" value. When several elements are so used, each having a different threshold energy, we can obtain information related to behavior of different energy groups in the experimental constraints. Ultimately, one may be able to construct a neutron (or proton) spectrum from these data.

Figure 5 shows a set of detectors arranged in the wooden troughs, ready for exposure at beam-axis positions in the shield array. Among the elements employed are aluminum, carbon, cobalt, copper, iodine, iron, magnesium, nickel, and titanium. These materials are used in the form of 4-in.-diam discs, of thickness from 1/32 to 1 in. With one exception we observe the γ-ray activity of radioisotopes produced during irradiations; this exception is carbon. Here we use the carbon a plastic scintillator, and detect the positron decay directly inside the scintillator. From all other materials, we obtain multichannel γ-ray spectra with a sodium iodide crystal scintillation spectrometer. Spectra are studied during decay of the various isotopes until we can obtain quantitative results for each isotope of importance.

2. Attenuation Measurements

The shield structure existed for two months, and during most of that time it served as the external-beam backstop for a physics experiment. Much of the period was suitable for our purposes, and it was at such times that we developed a series of attenuation profiles within the array. Gold foils, aluminum discs, and carbon scintillators were so employed, to provide information about three neutron-energy groups. Detector activities were observed at every 4-ft depth, laterally from the

beam axis to the shield's edge at 1-ft intervals. From these data we have constructed detailed radiation profiles for all positions inside the shield array, as viewed by these three detectors.[7] Results are discussed in detail in our later presentation, and will not be described further in this one.

3. Neutron Spectra

Several kinds of useful results were expected from this experiment. We were most interested in the neutron component of the radiation produced and propagated through the shield array, because this component usually determines the shielding requirements for high-energy accelerators. The use of activation-threshold detectors, within the formalism developed by Ringle,[1] held good promise for obtaining neutron-spectrum information.

Bevatron experimental conditions impose two new problems on the neutron-spectrum calculation method. The first of these is the presence of protons with energies capable of initiating some of the activation reactions. The second is the presence of both neutrons and protons with energies far beyond the range for which the method was initially intended. Direct application of Ringle's formalism to our Bevatron data was unsuccessful, that is: meaningful neutron spectra could not be obtained from threshold detector activations.

During his stay with our group, Kohler[2] concentrated on these problems, and was able to incorporate reasonable solutions for them into a modified version of Ringle's program. He could then derive neutron spectra at some positions within the shield array for the energy interval 2 to 30 MeV. We draw freely from Kohler's paper in the following discussion. The important changes and improvements introduced by Kohler are:

1. Use of experimental reaction cross sections in place of those calculated from the continuum model of the nucleus;
2. calculation of the amount of activation in threshold detectors caused by neutrons with energies greater than 30 MeV;
3. solution for the spectrum from the set of integral equations by a least-squares technique.

The use of experimentally determined reaction cross sections is largely self-explanatory. We show examples of cross section curves in Figs. 6 through 12; the first six of these were used in calculations of the neutron spectra shown in Figs. 13 and 14. We observe that the continuum-model calculations did not always agree with experimental data; in fact, there was often serious disagreement between the two results. Figure 12 shows an example of this sort of disagreement. Open circles are experimental data points, the solid line represents the shape chosen by Kohler, and the dashed curve represents the shape derived by the continuum-

model calculation. Our example illustrates one of the cases of greatest disagreement; however, this general problem exists for most other reaction cross sections, and use of experimental data exclusively has seemed the best choice. Even so, we found that somewhat arbitrary choices had to be made in cases of conflicting data. Data were sometimes very sparse and occasionally almost nonexistent. As a result of these factors, a certain amount of artistic selection has entered into the values we now employ. Reaction cross-section information is not nearly adequate for the potential of our method, particularly for the energy region above about 14 MeV; cross-section information is almost nonexistent for neutron-induced reactions above 30 MeV.

Calculations of the activations caused by particles with energies greater than 30 MeV is a very important item, simply because a significant fraction of detector activation at shield array sites may be due to these particles. Failure to make this correction will cause distortion in the calculated spectrum. Our correction scheme involves the use of Be^7 production in carbon (polyethylene) as the experimentally determined high-energy activation quantity. We assume a reasonable shape for the high-energy portion of the neutron spectrum, and also estimate the threshold detector cross-section shapes in this high-energy region. Both estimates are then combined with the Be^7 data to give a value of the correction for activation at energies greater than 30 MeV. Note that any errors in these corrections will be reflected as errors in calculated spectra. The need for high-energy cross-section data is clearly evident here. In all cases, it has been necessary to use proton-induced reaction cross sections, along with the assumption that neutron-induced reaction cross sections are of comparable magnitude, to create neutron cross section data; neutron data are nonexistent.

The solution methods developed by Ringle involved matrix inversion in the calculation procedure. This operation is very sensitive to any errors or inaccuracies in the experimental data that serve as input information; such errors can easily cause solutions to become so unstable that they are meaningless. Bevatron experimental data contained errors; furthermore, cross-section values were not accurately known. Solutions for neutron spectra were found to be unstable and without obvious physical significance.

Kohler modified the spectrum calculation procedure, and avoided the problems associated with matrix inversion by abandoning the solution method that required such operations. Instead, we use a scheme that seeks the best fit, in a least-squares sense, between "trial" neutron spectra and measured activations. The trial spectrum that most closely matches experimental activation data is then taken to be the neutron spectrum; this solution is achieved by a process of iteration. We impose a condition, as a means to stabilize the solution, that trial fluxes must everywhere be positive. Trial spectra are given either of two general

forms: a step-function representation, or a polygonal representation. The number of threshold reactions used in a calculation can be equal to, or greater than, the number of steps or segments in the solution. Use of more reactions than solution points can serve to improve precision of a solution; this technique can also show the presence of errors in either activation measurement or cross-section data, although no distinction can be made between the two types of error in a single spectrum calculation.

The least-squares method cannot reveal spectral detail so clearly as Ringle's matrix-inversion methods. However, it does give meaningful solutions from Bevatron data; these solutions are stable in a mathematical sense, and do not dissolve into incoherence when perturbations (errors) are purposely imposed on input data. Solutions also have a reasonable appearance in the context of physical reality.

We now turn to these results. On Figs. 13 and 14 we show log-log plots of step-function solutions for neutron spectra at four off-axis positions; data for these graphs are also presented in numerical form, as Table 3. Straight lines drawn through each spectral set are seen to represent reasonable fits to the data, with a possible exception at the position designated 8'-4'. (Here we mean a position at 8-ft depth located 4 ft off the beam axis.) Numerical values for slopes of the lines are indicated, and we conclude that the neutron spectral shape depicted by these results is consistent with a 1/E number-vs-energy relationship over the energy range 2 to 30 MeV. Such a spectral shape is expected from our general concept of neutron interactions in concrete shielding.

All neutron spectra shown in Figs. 13 and 14 are from locations within the shield array; however, all locations are off the beam axis. The correction for high-energy activation will be largest along the beam axis, and it is significant that beam-axis locations do not give meaningful spectral information at this time. We believe the reason lies in our inability to make the proper corrections for high-energy activation: large errors in large corrections make the method unworkable. If high-energy reaction cross-section data were available, we might be able to retrieve the situation to obtain beam-axis spectra, in addition to results now in hand.

Parts of this text appeared originally as a UCRL report (Alan R. Smith, Joseph B. McCaslin, and Michael A. Pick, Radiation Field Inside a Thick Concrete Shield for 6.2-BeV Incident Protons, UCRL-11331, Sept. 1964), a report that dealt mainly with attenuation measurements. The neutron spectral information is new, and was obtained by calculation methods not available when that report was issued. We are still engaged in data analysis from the experiment, and plan to issue a revision of the report, to include all useful results computed since the original issue date.

We are somewhat dissatisfied with results of the γ-ray spectroscopy that served as input date for neutron spectrum computation. A number of γ-ray analysis problems would be greatly reduced, or even eliminated, if a lithium-drifted germanium crystal were used as the spectrometer detector. We also note that the attenuation profiles, discussed in our second presentation, are not so precisely related to each other as we had hoped. Nothing can be done about these circumstances, short of performing the experiment again. There is considerable interest in such a project, especially in view of shield design problems raised by study of construction of higher-energy accelerators. If we do repeat the experiment, it will be as part of a larger effort, an effort that includes study of different shield materials as well as an investigation of shield behavior at larger angles with respect to the "target." Our present experience should serve as a valuable aid to successful execution of this larger experimental program.

D. Improvements to the Method

There are a number of improvements to be incorporated in our technique; we will discuss several of these items, because they are closely related to some of the problems described earlier.

We have used a 100-channel PHA to acquire all spectra used in this work to date; consequently, we must either observe a fairly narrow energy interval if we wish to utilize the full resolution capability of our NaI(Tl) crystal, or we must sacrifice resolution in the interest of obtaining spectral information over a wide interval. Neither is a happy compromise. Some of the difficulties we encounter in our method of spectral analysis are related to the fact that we do not observe γ-ray peaks with energies above 2.1 MeV. We note that digital computer programs work more smoothly when input spectral data do not contain sharp peaks. A larger-capacity PHA is clearly indicated, one with which we can record the entire γ-ray spectrum in one run, and at the same time achieve finer detail in its structure. Such equipment, a 1600-channel PHA, is a recent acquisition, and will be used for future threshold detector spectroscopy work. We will view the spectral region between 0.1 and 4 MeV in single runs, alloting either 400 or 800 channels to each spectrum. We are just now becoming acquainted with the new PHA, and should soon be applying it to this work.

Another problem concerns the gain stability of our spectrometer system. Digital computer analysis demands either that gain be kept constant or that instructions be provided to describe the extent of gain shift. We prefer a solution that maintains constant gain. It is well known that a major source of gain instability is the photomultiplier, and several schemes have been developed to compensate for this factor. However, gain changes can occur at other points in a system, and there are reasons

to prefer a constant photomultiplier voltage, while correcting for all gain shifts elsewhere. Such a device has been developed at LRL Berkeley,[8] and is used widely in Nuclear Chemistry research programs. In essence, we insert a variable-gain amplifier into the spectrometer system, and use address information from the PHA to correct for any gain shift. The unit analyzes this information in a digital mode and so is not dependent on count rate for effectiveness in control. The system is also adaptable for use with the high-resolution Ge(Li) γ-ray detectors, because it does not exercise control via variation of high voltage, but by gain change in an amplifier that can be an element common to all pulse-type detector spectrometer systems.

The digital gain stabilizer actually achieve its purpose by keeping a selected peak in the spectrum at a specified position. Most of our γ-ray spectra, especially those from medium-Z elements, contain a relatively intense positron-annihilation peak. We propose to lock onto this peak for stabilization purposes whenever it is present as a sufficiently distinct spectral feature; a standard stabilization procedure is then employed as widely as possible. A digital gain stabilizer will soon become an integral part of our spectrometer system.

We do not intend to incorporate a zero-shift correction into our spectrometer system. If such correction is required, it can be derived from gain-stabilized PHA data by testing whether peaks with known energies are separated by the correct channel intervals. We will deal with this matter if it becomes a real problem.

We show Fig. 15 in the context of improvements to be incorporated into our technique. The peaks shown here are meant to simulate the performance of a lithium-drifted germanium γ-ray detector; they belong to three scandium isotopes that may be produced from bombardment of natural titanium with neutrons of various energies. All three isotopes are produced when incident neutron energies are higher than 20 to 30 MeV, a situation obviously encountered at the Bevatron. The three different intensity levels serve to identify those peaks belonging to each decay scheme, and are shown at relative heights that might be observed shortly after a several-hour irradiation. Peak shapes are hypothetical, but are drawn to have resolution (full width at half-maximum) of 5 keV, a reasonable value for a Ge(Li) detector at these energies.[9] Each peak is clearly resolved from its neighbors, although the 1120-keV peak could merge into the 1160-keV peak if the latter were at much higher than the assumed intensity, or if resolution were considerably degraded. We see that it may be possible to observe quantitatively all γ-ray lines shown here in a single analysis using a Ge(Li) detector, in marked contrast to the repetitive analysis method necessary with the NaI(Tl) scintillation crystal. Such a repetitive series, shown in Fig. 2, serves to illustrate the point. Use of a Ge(Li) detector is possible for only relatively high-activity samples, because of the small size of these detectors--and thus, their

low efficiency. However, much of the Bevatron analysis work would have qualified for this category, so the technique is immediately useful.

Table 4 lists some characteristics of the dominant reactions in titanium leading to the three isotopes whose γ-ray spectra appear on Figs. 2 and 15. Several other reactions on titanium are listed on the table; estimated practical threshold for each reaction are given. We see that titanium is potentially a very useful threshold element. Neutron reactions with thresholds of about 1.5, 3, 5, and 14 MeV are available. The reactions $Ti^{47}(p, \alpha)Sc^{44}$ and $Ti^{48}(p, n)V^{48}$ are potentially useful indicators of proton flux.

We recognize that the listed scandium activities are not so simply related to single titanium isotopes as Table 4 might imply, especially when incident particles have energies of several tens of MeV or greater. Thus the actual use of titanium for neutron spectral measurement may entail additional problems; these problems stem mainly from the existence of several abundant stable titanium isotopes. However, γ-ray spectral analysis is straightforward, and no more difficult than we indicate here. We offer titanium as an example of the spectral complexity that is also encountered with other medium-Z elements such as iron, nickel, cobalt, and copper--elements that are needed for this neutron spectroscopy method.

We have not made extensive use of coincidence techniques for γ-ray spectral analysis. Such techniques could be very effective for resolving components in some complex spectra acquired with NaI(Tl) crystals; these techniques may be even more powerful when a mixed pair of detectors is used--one NaI(Tl) crystal and one Ge(Li) crystal. Our new PHA is large enough and has enough operational flexibility so that these potentially useful methods can be explored.

The complexity in these γ-ray spectra is due largely to the class of events termed "spallation" reactions. When we have high-energy incident particles, spallation reactions may be as important as the selected simple reactions (that is, they may have similar magnitude cross sections). Spallations may produce the same activity we wish to study, may produce activities that interfere with observation of a desired activity, or may produce activities that are easily observed as separate features in the complex γ-ray spectra. These reactions usually have relatively high threshold energies, and it is this characteristic that marks them as potentially useful to our purpose. If we knew spallation-reaction cross sections more exactly, we could not only make more accurate corrections when they cause interference in γ-ray analysis, but we could also employ them as bona fide members in that group of threshold reactions used for the spectroscopy itself. Examples of prominent spallation reaction products are Mn^{52} and V^{48} from copper, nickel, cobalt, and iron; also Co^{58} from copper. Unfortunately, detailed cross-section information for these reactions is all but nonexistent.

We can summarize these paragraphs as follows. In order to use the medium-Z elements to their full potential, we require two advances beyond our present position. The first, a high-resolution γ-ray detector, has recently become available in the form of the Ge(Li) crystal detector. Such detectors are small in comparison with easily obtainable large-size NaI(Tl) crystals; however, they would now satisfy analysis requirements for high-activity samples. We are preparing to put such a detector into operation, along with the new 1600-channel PHA and a digital gain stabilizer.

The second requirement, detailed cross-section information for the reactions, is almost totally nonexistent for titanium throughout the entire energy range of interest, and is largely nonexistent for other elements at neutron energies above ≈ 20 MeV. Without this cross section data, we are forced to throw away (or ignore) most of the information contained in γ-ray spectra. The knowledge required here is fundamental nuclear reaction data, the sort of thing that is appropriate to thesis research projects. Our success, using the limited amount of information now available, is clearly evident; it should be just as evident that additional information will contribute significantly to increased success. We suggest that the double inducements--appropriateness of topic, and utility of results--should serve as strong stimuli to research efforts in this area of comparative ignorance.

IV. NEUTRON SPECTRA OUTSIDE THE ACCELERATOR SHIELDS

The next series of measurements has been made as part of an effort to clarify our understanding of the fast-neutron energy spectrum that exists outside an accelerator shield. Past experience around the Berkeley accelerators has always supported the conclusion that this spectrum had a shape quite similar to the cosmic-ray neutron energy spectrum, as reported by Hess, Patterson, and Wallace.[10,11] The evidence is in part that of experimental measurement of the spectrum itself; it is also based on evaluation of performance of shielding that has been designed to provide a particular attenuation factor if such a neutron spectrum did, in fact, exist within the shield structure. We cite evaluation of the improved shield at the Bevatron, described earlier in this paper, as an example; shield design is reported by Moyer.[26]

Some recent measurements from CERN,[12] BNL,[13] and HASL[14] suggest that with certain shielding conditions at multi-BeV accelerators, the spectrum may be much richer in high-energy neutrons than we would expect. Although it is not clear how these particular shield conditions can be precisely described, it does appear that one requires a relatively thin shield and a nearby target. These results are puzzling at present, and have acted as one stimulus for the measurements now described. Great interest in design of higher-energy accelerators has been another strong incentive; and finally, our own interest in such matters has naturally brought about all the preparations necessary for actual performance of the study.

A. Description of Detectors

We employ the mixed system of threshold detectors here; this system includes moderated BF_3 counter or foil, aluminum disk, carbon scintillator, and the bismuth fission counter. We have either two prompt counters and two activation elements, or one prompt counter (when a moderated foil is used) and three activation elements. Before we discuss the use of data from these detectors in spectral measurements, we will describe briefly the nature of the data itself.

The BF_3-filled proportional counter is a familiar device whose operation is straightforward. There is no need to discuss such well-known matters here, and we will comment only on the problem of count loss. The magnitude of count loss due to high rate of arrival of information at the detector can be determined by intelligent viewing of amplifier output pulses on an oscilloscope. If count-loss problems cannot be solved, we use a moderated foil in place of the moderated BF_3 counter. Such foils, of either indium or gold, are subsequently analyzed for induced activity with an end-window methane-flow proportional counter; this counter has an absolute detection efficiency of about 35% for the β particles emitted by our 1-in.-diameter foils.

We note that count loss in the BF_3 counter has been almost eliminated as a problem for all Bevatron stations considered here. McCaslin reports[15] such details in another paper of this symposium. The essential point is that we are able to achieve stable operation of a high-sensitivity BF_3 counter while enjoying a pulse-pair resolution time of about 0.1 μsec. Thus we can record several hundred counts during a 1-msec beam burst without incurring significant count loss.

We observe the decay of Na^{24} in aluminum disks as evidence of neutron-induced reactions; in fact, we assume all Na^{24} is produced by incident neutrons. Aluminum disks, 8 in. in diameter by 1 in. thick, are analyzed for Na^{24} content with a γ-ray scintillation spectrometer, which uses an 8-in.-diameter by 4-in.-thick NaI(Tl) crystal as a detector and a 100-channel pulse-height analyzer for data acquisition. A carefully shielded counting facility provides the low-background environment required for this analysis work. Typical spectra are shown on Fig. 16. The Na^{24} spectrum appears as the upper curve; it represents data from an aluminum disk containing relatively high Na^{24} activity, so that the shape is not distorted by background count contribution. The lower curve shows an appropriate background (BKG) spectral shape: data obtained from an unexposed disk. The original data were acquired during a 1300-minute run, and are shown here at magnitude appropriate to a 220-minute run time.

We observe C^{11} decay inside plastic scintillator as evidence of neutron-induced reactions.[16] Here again, we assume that neutrons are responsible for all the observed activity. The scintillators are 5-in.-diameter by 5-in.-high right circular cylinders. The internal decay

radiation is studied with a spectrometer system that uses a 100-channel pulse-height analyzer for data acquisition. Typical spectra from this system are shown on Fig. 17. The solid curve represents response from a scintillator irradiated for 1 hour at a Bevatron location where the moderated BF_3 counter reported a fast-neutron flux intensity of 30 n/cm^2-sec. The actual PHA data run lasted 10 minutes; the curve is shown shifted down-scale one order of magnitude from its original position, to achieve an ordinate scale of c/min-channel. The dashed curve depicts the response observed from an unexposed scintillator (the same scintillator before exposure); this curve is based on a 1000-minute run, normalized in terms of c/min-channel. Vertical bars indicate the spectral region we accept as valid C^{11}-decay information; the interval was selected to maximize our ability to detect C^{11} decay with the present background count conditions.

The bismuth fission counter is a large-area parallel-plate ionization chamber;[17] it is actually built of multiple plates coated on each side with a thin layer of bismuth so that there is a total of 60 grams of active bismuth. We operate the chamber as a pulse counter, observing fission events as signals which result from fast collection of electrons. Such signals are similar to those produced by proportional counters, although they are much smaller. After suitable electronic amplification, these pulses are sorted and recorded on a 10-channel pulse-height analyzer. We show typical data from this counter on Fig. 18; note that these are integral bias curves, not differential curves as for the previous two examples. The steeper curve represents data taken at a Bevatron location from an overnight run; actual data points, divided by a factor of 4, are shown. The dashed line extending to zero bias indicates the nature of the zero-bias extrapolation required to match calibration conditions. The second curve, with relatively shallow slope, represents data from a 3-minute run on the internal Cf^{252} fission source. Such data are taken frequently to verify the correctness of gain for the entire system, including the fission counter.

B. Relationships between Detector Response and Neutron Spectra

We obtain spectral information for the neutron energy range extending from about 0.02 MeV up to 6.2 BeV, the full energy of the accelerator-produced primary beam particles. Detailed spectral shape can be obtained only when detectors have threshold energies spaced throughout the energy region of interest. Our highest threshold, about 50 MeV for the bismuth fission counter, is far below the primary particle energy, and so this system can delineate only the broad character of a neutron spectrum. However, knowledge of reaction cross sections (or detector response) up to the primary energy allows the construction of rather narrow limits on the possible (and reasonable) spectral shape.

We have explored the relationships that exist among detector response, or reaction cross section, detector count rate, and neutron spectral shape. A digital computer program assists our study, and is arranged so that input parameters can easily be varied. The computer program

actually works in the reverse direction with respect to the problem; this approach has been taken for reasons of mathematical simplicity. We assume a neutron spectrum, and also assign values to detector response functions. The program then computes detector count rates belonging to these chosen parameters. In practice, it is most meaningful to hold one kind of parameter constant (say the response functions) and vary the other parameter. We might vary the assumed neutron spectrum until we have achieved a set of computed count rates that match a set of observed count rates; this is an example of determining the neutron spectrum. We might also vary the neutron spectrum in some systematic ways to explore the nature and extent of count rate changes.

The other case, variation of response functions with a fixed neutron spectrum, is also of great interest. This kind of variation permits one to explore the changes in computed count rates that would result from errors in response functions, i.e., calibration constants and reaction cross sections. As we are well aware, reaction cross section values are imperfectly known, and it is very important to understand the effect such inaccuracies can have on our results.

We present some results obtained from the computer program. We have not introduced sharp variations--variations that seem unreasonable in terms of physical principles or known-valued parameters--in either assumed neutron spectra or response functions. Our purpose is not to demonstrate the efficacy of the method in dealing with all possible extremes, but is rather to map its performance over a modest region within which we believe the true situation resides.

As a first example, we take fixed values for all response functions, and investigate the behavior of computed count rates as we perform variations on the neutron spectrum. We use the 1/E shape for the basic differential neutron energy spectrum--a distribution that contains equal numbers of neutrons in each energy decade. We superimpose a flat energy distribution on this spectrum one decade at a time, starting with the interval 0.02 to 0.20 MeV, to simulate a broad peak lying within the appropriate decade. The lower limit of 0.02 MeV is chosen because dose contribution at energies below this point is unimportant. The 1/E spectrum is shown on Fig. 19 as a heavy straight line, and superimposed flat distributions are indicated by triangular areas bounded by lighter lines. Numbers appearing inside these areas are then used as keys on the horizontal scale of Fig. 20. This figure shows computed count-rate changes for each detector when we perform the successive spectral variations. Each detector count rate has been normalized to unity for the basic 1/E shape. Smooth curves are drawn through computed points, to emphasize contrasts among detector response functions.

The greatest contrast exists between moderated BF_3 and BiF counters, as one would expect. These two detectors report information from almost completely separate regions of the neutron energy spectrum,

and so should be most sensitive to the spectral changes we wish to observe. Carbon and aluminum show intermediate behavior. We note that aluminum does have a response peak in region 3, the 2.0-to-20.0-MeV decade, but that its response function is also effective at all higher energies. The high-energy aluminum response is already important at a spectral energy end point of 6.2 BeV; it will be increasingly important as higher end-point energies are encountered. In short, we cannot assume aluminum is sensitive within only a narrow energy region. As we would expect from their simple cross-section shapes, carbon and bismuth are almost equally affected at very high energies; they differ mainly to the extent that their thresholds occur at different energies.

For our next example we take a fixed neutron spectrum, again the 1/E distribution, and perform variations on the response functions of detectors; computed count rates are examined to learn the extent to which errors in calibrations or cross sections can influence our results. We will assume that moderated BF_3 counter calibration and response function are well known,[10] so we do not perform variations for this detector. (Response of the BF_3 counter at energies above 14 MeV is taken to be proportional to corresponding values for the hydrogen total cross section.) The main question concerns behavior of aluminum, carbon, and bismuth fission detectors with respect to these variations.

Response-function variations for aluminum, carbon, and bismuth are listed in Table 5; these values are cross sections in millibarns (mb) for production of the observed reactions or activities. In each case, preferred values are listed first, and variation sets appear in succeeding columns. Preferred values are also shown in graphical form on Figs. 21 and 22. These curves are based on recent compilations by Bruninx[18] and Cummings,[19] and recent work by De Carvalho, et al.[20] We list computed count rates from the 1/E spectrum for each complete set of response functions; we also show the percentage change observed for each variation set relative to values obtained from the preferred set. The last column contains the preferred set of relative values for the moderated BF_3 counter response function.

We draw attention to the following items. The value of the aluminum cross section is maintained constant at 100 mb in the 6-to-20 MeV energy region. If we then vary the value for the flat portion of the high-energy cross section from 7 to 15 mb, we observe only a decrease of 12% and an increase of 13%, respectively, in count rate. Data not presented here also show that details in shape of the cross-section curve that joins the peak region to the flat portion are of no practical importance. For carbon, the presence or absence of a peak of reasonable magnitude just above threshold has little effect on computed count rates. By similar tests, one can demonstrate that reasonable errors in values for reaction energy thresholds produce small changes in computed count rates. For example, if we assume the carbon cross section to be zero everywhere below 60 MeV, our computed scintillator count rate decreases only about

20%. We are attempting to observe only broad spectral shapes, not sharp details, and so we can view a 20% change as a minor one.

These observations are valid for the 1/E spectral shape when this distribution extends to energies far above those at which reaction cross sections exhibit rapid change, or sharp structure. The shape we deduce for the Bevatron spectrum does not depart widely from a 1/E distribution until we reach the vicinity of 1 BeV; thus the above remarks should be valid for our work at the Bevatron. Were the spectrum extended to higher energy, as a higher-energy accelerator, sensitivity of detector response to changes in cross-section fine structure would be reduced even further.

In the third example, we use what we consider to be the most reasonable values for response functions, and compare count rates computed for several different neutron spectra with the count rates actually observed at the Bevatron. These spectra include: a flat energy distribution, the 1/E energy distribution, the experimentally determined cosmic-ray neutron energy spectrum, [10, 11] and the neutron energy distribution that provides a good fit for the Bevatron experimental data. The latter three spectra are shown on Fig. 23.

This Bevatron spectrum is essentially a combination of the 1/E distribution at low energies, and the cosmic-ray distribution modified for a 6.2-BeV energy end point; the two basic shapes are joined smoothly in the vicinity of 10 MeV. The spectrum shown here represents an average derived from five measurement sets, all obtained at the outer surface of the Bevatron main shield. These stations were located in the vicinity of a thick internal target in the Bevatron south tangent tank, at angles that ranged from 90 to about 45 deg forward with respect to the beam-target line. Shield thickness varied from about 5 ft minimum to about 14 ft maximum. For aluminum, carbon, and bismuth the spread of values among individual sets is small relative to the averages shown here: all lie within + 15% of the averages. Moderated BF_3 counter response shows a wider range, with one value about 50% above, one about 50% below, and the other three within ± 15% of the average value. Sensitivity to low-energy scattered neutrons is an important contributor to this behavior of the BF_3 counter.

The performance of our four detectors is shown graphically on Fig. 24, where we plot their response to the different neutron spectra. All detector response values are shown relative to that response observed in the Bevatron spectrum; the Bevatron response is taken to be unity for each detector. An additional normalization places all BF_3 values at unity, to emphasize contrasts among high-energy detector response characteristics. The horizontal scale has no physical significance beyond that of arranging detectors according to reaction energy thresholds. Note that aluminum, carbon, and bismuth responses to the cosmic-ray spectrum are at least a factor of 2 lower than those for the Bevatron; also, that detector responses to the 1/E spectrum are at least a factor of 2

higher than those for the Bevatron. The important point is that we can tell differences among these spectra rather easily. Stated in another way, we observe that the method is sensitive to broad spectral differences, and is able to make clear choices without requiring extremely precise input data.

C. Relationships between Neutron Spectra and rem Dose

We comment briefly on the relative biological hazard associated with each of the four spectral distributions. We use NBS Handbook 63[21] and ICRP[22] recommendations for conversion of neutron flux intensity into rem dose for energies up to 10 MeV.

Although conversion of flux to dose at energies above 10 MeV is somewhat a matter for conjecture, we accept the expression $30.2/E^{\frac{1}{4}}$ the flux of neutrons unaccompanied by secondaries that delivers 100 mrem in 40 hours, as a relationship that is based on reasonable calculations.[23,24] We use the rem data and operate on a spectrum to find the dose contributed in each energy interval. These contributions are then summed, starting with the lowest energy interval, and the summation is normalized to a value of 100% for the complete spectrum. We can now construct a curve to show percentage of total dose contributed below any given neutron energy. Results of these operations on our four spectra are shown in Fig. 25. In all but the flat spectrum (an unrealistic distribution), roughly 1/2 to 4/5 of the dose is delivered by neutrons with energy less than 60 MeV: values from the curves are 45% for 1/E, 60% for Bevatron, and 83% for cosmic ray. We can also use spectral shapes and RBE data to compute values for rem/neutron. We find the highest value to be 7×10^{-8} rem/n for the flat spectrum, and 3.3×10^{-8} rem/n for the cosmic ray spectrum: only a factor of 2 difference for these strikingly dissimilar spectral shapes.

D. Results at 184-Inch Cyclotron

The mixed system of threshold detectors has also been used at the Berkeley 184-inch cyclotron; we cite one example of its application at this accelerator. We selected a station at the outer surface of the main accelerator shield, where detectors were located in a forward direction with respect to high-energy particles emerging from the cyclotron and were shielded by a 15-ft thickness of concrete. The accelerated particle beam consisted of full-energy (730-MeV) protons.

Results of this exposure are consistent with the Bevatron results described previously. In particular, count rates from moderated foil, aluminum disk, and carbon scintillator were almost identical in relative terms to these same detector responses observed in our averaged Bevatron result. The bismuth fission counter showed a somewhat higher relative count rate at the cyclotron than at the Bevatron; even so, the

cyclotron results indicate a spectral distribution whose slope is steeper than 1/E at high energies.

Let us examine the cyclotron results in greater detail. The moderated foil indicated a fast neutron flux value of 75 n/cm^2-sec, while the bismuth fission counter reported a value of 18 n/cm^2-sec. As we have already demonstrated, these two detectors respond to (nearly) separate spectral regions; we will now assume they do respond to completely separate regions. Consider the moderated foil response to lie within the region 0.02 to 20 MeV, three decades of energy; also, consider the bismuth fission counter response to lie in the region 50 to 700 MeV, slightly more than one decade. By definition, a 1/E differential spectrum contains equal numbers of neutrons in each decade; therefore these two detectors are seen to prescribe the existence of very nearly a 1/E spectrum. This situation is indicated because the moderated foil gives approximately three times the flux value shown by the fission counter, from a response characteristic that extends over three times the range of energy. In fact, we would infer a slightly steeper slope from our observed flux values and the assumed response regions.

We have also shown that in a 1/E spectrum, about 50% of the neutron dose is delivered by neutrons of less than 60 MeV; thus the below-60-MeV percentage at the cyclotron station should be somewhat higher, because the spectrum falls more rapidly than 1/E, and there is a direct relationship between steepness of slope and this dose parameter.

For the 1/E spectrum, our calculations predict that the dose per neutron is about 4.6×10^{-8} rem/neutron. When we use the two-counter method (moderated BF_3 counter and polyethylene-lined counter) at this station,[25] the experimental data indicate a value of 4.4×10^{-8} rem/neutron. Here again we see a consistent pattern reported by widely different neutron detectors. Such performance offers additional strong confirmation regarding the applicability of our detection systems and measurement techniques for use at high-energy particle accelerators. As we have stated before, the kind of data reported by these detectors is useful for both biological hazard and shield design problems. This point cannot be emphasized too strongly.

E. Use of Detectors in Low-Intensity Fluxes

The method can be applied over a wide range of neutron flux intensities. At locations outside accelerator shields, the problem is usually that the intensity may be too low (rather than too high) for successful measurement. It is in the context of low-intensity measurements that we have recently made greatest progress; to this area we now turn our attention.

A moderated foil or BF_3 counter can easily be made to provide the required sensitivity for low-intensity measurements. Our large bismuth fission counter registers about 1 count/sec when immersed in a uniform neutron flux intensity of 57 n/cm^2-sec, at 220 MeV neutron energy; thus a flux intensity of 1 n/cm^2-sec at energy well above threshold will produce about 60 counts/hour. We require the order of 200 counts per run from the bismuth-fission counter in the interest of statistical value of results. If we then assume a ratio of 10:1 between BF_3-indicated total fast neutron flux and bismuth fission neutron flux, the lower limit on flux intensity for a 1-hour exposure is about 30 n/cm^2-sec, as measured by the BF_3 counter.

A 1-hour exposure is about three half-lives for the 20.4-min C^{11} activity observed in carbon scintillators, and is considered to be close to the maximum allowable exposure time for typical irradiation conditions. If carefully controlled constant-intensity conditions can be guaranteed, then there need be no limit on scintillator exposure time, but we usually are unable to specify such conditions, and so impose this somewhat arbitrary time limit. We consider a 1-hour exposure to be compatible with scintillator activity half-life, if we can be certain that irradiation conditions remain reasonably constant during this interval. An interval during which accelerator beam magnitude fluctuated in a random fashion around one particular value would be an acceptable exposure condition; an interval during which the beam intensity changed erratically and attained a significantly different value would not be an acceptable irradiation condition.

The carbon scintillators used for this work are 5 in. in diameter by 5 in. thick, weighing about 1700 grams.[16] Our experimental calibration at 220 MeV neutron energy and a calculation using a reaction cross section value of 22 mb indicates a count rate of 104 counts/min from an immediate analysis following a long exposure at intensity 1 n/cm^2-sec. If we use the BF_3 flux intensity of 30 n/cm^2-sec, and assume a carbon flux of 5 n/cm^2-sec, we observe a count rate in excess of 400 c/min in the scintillator. This count rate is easily measured with good precision.

The aluminum discs are 8 in. by 1 in. thick, and weigh 2.2 kg each; the NaI(Tl) crystal used for Na^{24} assay is 8 in. in diameter by 4 in. thick. The large size of this system is necessary because the 1-hour exposure is quite short in comparison with Na^{24} half life, 15 hours. A 1-hour exposure produces only about 4.5% of the equilibrium amount of Na^{24} in a disk, and so our potential sensitivity must be much greater than can be used in the present context.

At calibration neutron energy, 14 MeV, irradiation of a disk to equilibrium in a constant flux of intensity 1 n/cm^2-sec will produce 70 counts/min in our γ-ray scintillation spectrometer system. We use the γ-ray energy interval 1.29 to 2.90 MeV to define Na^{24} activity. This interval includes the two prominent γ-ray peaks and the intervening

continuum; it was selected to maximize the sensitivity for Na^{24} detection in our spectrometer system.

We again select the 30 n/cm^2-sec total fast neutron flux intensity, and assume 1/5 of this flux to be the equivalent 14-MeV flux. We then observe about 16 counts/min due to Na^{24} decay if a disk is counted soon after the 1-hour irradiation. At a background (BKG) count rate of 95 counts/min, we can determine this activation to ± 7% in a 100-min count period.

From this brief description, it should be clear that the method is useful for flux intensities existing in areas that may be occupied a significant fraction of the time. This comment pertains to the 1-hour simultaneous exposure. When we can permit longer exposures for aluminum disks and the bismuth fission counter, much lower flux intensities can be studied successfully.

We cite the example of aluminum in this context because it is the activation element which has been most thoroughly studied in terms of low-flux measurement capability. The calibration at 14 MeV neutron energy gives a value of 70 counts/min in our Na^{24}-assay interval when a single disk is irradiated to equilibrium in unit neutron flux. If five disks were irradiated in this manner and then counted stacked together on the 8-in.-diameter crystal, we would observe about 150 counts/min. Extrapolation of some recent tests with different sizes of disks indicates that we might achieve a count rate of about 400 counts/min if five discs of 16-in. diameter were analyzed together. Note that the BKG has not increased as we increase the amount of activation element (assuming, of course, that the disks contain no natural radioactivity); thus the count-rate increase is all clear profit, so to speak.

We can now estimate the lower limit for measurable flux, using the above values and a nominal BKG rate of 100 counts/min. Consider a count period of 1000 minutes closely following long exposures to 14-MeV neutrons. An intensity of 0.01 n/cm^2-sec can be determined to ± 14% with a single disk, and to ± 7% with five disks, each 8 in. in diameter by 1 in. thick. Single disks of this size are used routinely; multiple arrays have been used for special situations. We consider this to be a practical system for flux measurement.

If we used 16-in.-diameter discs, five at a time, we could determine a flux of 0.001 n/cm^2-sec to ± 25% in the 1000-min count period. Such a measurement assumes the proportions of an heroic effort, but is by no means impossible.

Use of a pair of crystals instead of a single crystal would improve all performance characteristics; use of larger crystals would also provide a net gain. It does appear that the order of 0.001 n/cm^2-sec is close to the lower limit of measurable flux from a single irradiation and a single analysis period.

The most important aspect of this increased sensitivity is not the ability to measure such small fluxes from long irradiations, but is to be able to measure considerably higher fluxes from much shorter exposures. Compatibility with the 20.4-min C^{11} half-life is an important factor here. Accelerator beam time is always at a premium, and the capability of using short intervals of beam control greatly enlarges the scope of measurements we can undertake.

We have not attempted to develop extremely high sensitivity in any other activation element, except in carbon scintillators. The other threshold reactions described in the first part of this paper produce measurable activations when the 4-in.-diameter samples are irradiated for an hour in flux intensities on the order of 100 n/cm^2-sec, well above threshold. We are now studying the value of these reactions to the mixed system method, in an effort to determine which, if any, elements should be developed into very-high-sensitivity detectors.

F. Background Count-Rate Considerations

Our success in measurement of low-flux intensities (small induced activations) is related directly to our ability to provide a counting environment in which the BKG rate is both very low and very constant.[6] In fact, without such a BKG environment these measurements would be impossible. We will omit detail here, and simply state that the BKG count rates in our spectrometer detectors are constant within the statistical significance of frequent long BKG runs--that is, within a small fraction of 1%. Use of a carefully maintained spectrometer system with this counting facility then permits us to accept as valid information net count rates that are small compared with the BKG rate. Spectrometer runs that produce low net count rates are always done carefully, but such runs are usual rather than unusual in our work.

For aluminum disc analysis, low BKG in our 8-in.-diam by 4-in.-thick NaI(Tl) crystal is due entirely to the low-background counting facility and careful selection of low-activity components in the crystal-photomultiplier assembly. We have made a careful study of the observed Na^{24} γ-ray spectrum in relation to spectrometer background response. This study shows clearly that both the 1.37-MeV and 2.75-MeV total absorption peaks and the intervening continuum should be accepted when we wish to obtain the maximum information in a given counting time. This situation is true at all activity levels, and is particularly important for measurement of low levels. If we allow at least 30 min between exposure end and analysis start, no interference is likely to be encountered from any other γ-ray activities. A possible exception is Na^{22}, a 2.6-year-half-life isotope; however, Na^{22} activity will be negligible in comparison with the Na^{24} activity from any single exposure. Na^{22} activity is more properly viewed as a BKG problem; in particular, one must keep track of previous exposure history for disks that are to be reused.

Spectrometer BKG rate in the Na^{24} interval (1.25 to 2.90 MeV γ-ray energy) is 85 counts/min when no sample is present on the detector; it should remain at this value when unirradiated disks are counted. However, a single unirradiated disk increases the BKG rate to 95 counts/min, because of the presence of a small amount of thorium in the type 6061 aluminum alloy used for our disks. This is an unimportant difference in terms of increasing the magnitude of BKG, but must be known accurately when small activations are measured.

For the C^{11}-assay, we have been able to reduce BKG count rate in a 5-in.-diam by 5-in.-thick plastic scintillator from the previous value of 700 to 800 counts/min to the present low value of 125 counts/min. The improvement is due partly to use of the low-background counting facility, and partly to use of a 100-channel PHA for data acquisition. The PHA technique permits very precise and reproducible selection of an upper boundary on the pulse amplitude accepted as valid C^{11}-decay events, while at the same time excluding all larger-amplitude pulses that contain no C^{11} information. For all but the lowest-activity scintillators, a single PHA run can easily verify that the activity is C^{11}, verify that the system gain is correct, and check for the proper selection of an upper boundary of C^{11} events. As a direct consquence of this method, we can process more scintillators in less time and with greater precision than has been possible in the past.

Both detectors produce a net count response from an equilibrium exposure to unit flux at calibration neutron energy that is nearly equal to the respective BKG rates. For aluminum we have 70 counts/min compared with 95 counts/min; for carbon we have about 100 counts/min compared with 125 counts/min. The net count rates are also relatively large numbers in both cases. This is an important consideration when counting time is desired to be kept short, as in aluminum, or when half life is short, as in carbon.

G. Concluding Remarks

We call attention once again to the more or less accurate nature of this work. Neither cross-section values, detector calibrations, nor RBE values are known to desired precision, particularly at very high neutron energies. The purpose here has been to indicate some of the trends one can discern if we first agree upon values for these approximately known quantities, and then use them with reasonable models to study certain problems. We see that cross sections and detector calibrations need not be known exactly in order to study smoothly varying wide-range neutron spectra. We note that different spectral shapes can be clearly distinguished with our four-detector system, and that this work can be carried out successfully at "occupational" flux intensity levels. Our evaluation indicates that the Bevatron neutron spectrum is quite similar to the previously measured cosmic-ray neutron spectrum. Finally, we see that the dose per neutron is relatively insensitive to the spectral shapes likely to be encountered outside shields at a high-energy

particle accelerator.

Our use of this detector system has one important nontechnical aspect that should be mentioned. We find it most effective for three or four people to do the actual detector analysis, each person concentrating his effort on one particular detector. However, these people are simultaneously at work on a common project, and are led naturally to acquire familiarity with characteristics of all four detectors. The significant (and immediate) results achieved through such joint purpose serve as healthy reminders of the advantages that cooperative effort can provide. Too often we work in relative isolation, unaware of our colleagues' thoughts, accomplishments, and capabilities; it is quite beneficial to have frequent clear purpose for common effort, such as we describe here.

V. SUMMARY

At the Berkeley accelerators, we find the neutron component of the radiation field to be the most significant in terms of biological hazard; it is also the most useful component for shield design and evaluation purposes. It follows that we attach great importance to the study of characteristics of this neutron flux. The studies we have just reported, the application of two types of threshold detectors to neutron spectroscopy around the high-energy particle accelerators, are seen to be items central to our purpose.

We have obtained neutron spectral information with activation-element threshold detectors at the Bevatron, where 6.2-BeV protons were the particles incident on a thick concrete shield structure. The spectra were measured at locations inside this shield array--but only at locations that were not directly on the proton beam axis. Observed spectral shapes are consistent with a 1/E distribution over the energy range 2 to 30 MeV, and are in agreement with results acquired through use of our mixed system of threshold detectors. We have been unable to derive meaningful spectral results from detectors irradiated at positions along the proton beam axis, principally because we are not able to make proper correction for the fraction of detector activation that is caused by high-energy particles. The paucity of high-energy neutron cross-section data is the most serious obstacle to progress here.

Activation-element threshold detectors have also been used at the 88-inch cyclotron, where incident particle energies are less than 80 MeV; analysis of detector activation is much simpler here than at Bevatron particle energies.

We have discussed some problems that accompany the use of activation-element detectors. Problems associated with γ-ray spectrum analysis are described, and some solutions are suggested. We conclude that the most serious γ-ray analysis problems can be solved through use

of more sophisticated digital computer programs, the larger-capacity PHA, and (in some cases) high-resolution Ge(Li) γ-ray detectors. This work is now under way. The other major problem, the lack of reaction cross-section data, is a matter that cannot be so easily remedied. The requirement here is for basic nuclear reaction data, and will entail a considerable research effort for measurement of the important cross sections. This appears to be a long-range project, but is amendable to attack in many places at once, and would seem to be excellent thesis research material. We urge that such efforts be undertaken.

In our study of neutron spectra outside the shield but near a thick Bevatron target, we have shown how the mixed system of threshold detectors indicates a particular spectral shape. The observed neutron spectrum exhibits a 1/E shape in the energy region 0.02 to 10 MeV, and a somewhat steeper slope as the energy increases beyond 10 MeV. This slope is quite similar to that of the cosmic-ray-produced neutron spectrum, and appears reasonable in view of nuclear interactions that high-energy particles experience as they penetrate a massive concrete shield.[26-29] We indicate how the preferred spectrum may change if reaction cross-section values are incorrectly chosen, and demonstrate that such changes are small if the errors in these cross sections are reasonably small. We describe use of this system at the 184-inch cyclotron, where the observed spectral shape is again consistent with the description just given.

Results of these studies are consistent with our general concepts of shield behavior and neutron spectral distribution when high-energy accelerator-produced particles generate the radiation field. We see that threshold detectors are quite effective in providing information for the investigation of such phenomena over a wide range of flux intensities. We also see that lack of basic nuclear reaction data is one of the most serious limitations to more widespread and effective use of these detectors.

ACKNOWLEDGMENTS

Much of the information presented here represents the work of others at this Laboratory, both within and without the Health Physics Department.

Formal contributions are acknowledged in the accompanying list of references; however, informal contributions probably equal the listed ones in importance. Among the outstanding contributors in the latter category, to whom we give especial thanks are:

Joseph B. McCaslin, Alvin J. Miller, Michael A. Pick, and Lloyd D. Stephens, for radiation survey and threshold detector data taken at the Bevatron; Henry A. Dakin, for radiation survey data taken at the 184-inch cyclotron;

H. Wade Patterson, Ralph H. Thomas, and Roger W. Wallace, for work in connection with determination of the preferred shape for the Bevatron neutron spectrum;

Mrs. Nickey Little, for acting as our intermediary with the digital computers;

The Bevatron staff, for shield array construction, beam transport and monitoring, and efficient accelerator operation, during the shield array experiment; also, for their generally helpful and cooperative spirit shown toward all our work at this accelerator;

Particular appreciation is expressed to Burton J. Moyer, Administrative Head, Health Physics Department, who originally generated the climate within which the kind of work reported here could be accomplished; such appreciation is also expressed to H. Wade Patterson, who has maintained and further encouraged this climate in his supervision of our Health Physics work.

REFERENCES

1. J. C. Ringle, A Technique for Measuring Neutron Energy Spectra in the Range 2.5 to 30 MeV Using Threshold Detectors (Ph. D. Thesis), USAEC Report UCRL-10732, Lawrence Radiation Laboratory, October 11, 1963.

2. A. D. Kohler, Jr., An Improved Method of Neutron Spectroscopy Using Threshold Detectors (M. S. Thesis), USAEC Report UCRL-11760, Lawrence Radiation Laboratory, December 11, 1964.

3. W. W. Wadman, Shielding Attenuation of Neutrons from 80-MeV γ-Particle Bombardment of Elemental Tantalum, USAEC Report UCRL-16359, Lawrence Radiation Laboratory, October 4, 1965 (for Proceedings of American Nuclear Society Shielding Division; also submitted to Nucl. Sci. Eng.).

4. A. R. Smith, Some Experimental Shielding Studies at the 6.2-BeV Berkeley Bevatron, USAEC Report UCRL-16323 Abst., Lawrence Radiation Laboratory, August 2, 1965, also, Proceedings of this Conference.

5. P. M. Morse and H. Feshbach, Methods of Theoretical Physics (McGraw-Hill Book Co., Inc., New York, 1953), Chap. 8.

6. H. A. Wollenberg and A. R. Smith, A Concrete Low-Background Counting Enclosure (USAEC Report UCRL-11454, Lawrence Radiation Laboratory, June 15, 1964) Health Phys. (to be published).

7. A. R. Smith, J. B. McCaslin, and M. A. Pick, Radiation Field Inside a Thick Concrete Shield for 6.2-BeV Incident Protons, USAEC Report UCRL-11331, Lawrence Radiation Laboratory September 18, 1964.

8. M. Nakamura and R. L. La Pierre, A Digital Gain Stabilizer for a Multiparameter Pulse-Height-Recording System, USAEC Report UCRL-11494, Lawrence Radiation Laboratory June 16, 1964.

9. D. A. Shirley, Applications of Germanium Gamma-Ray Detectors, Nucleonics 23[3]; 62 (1965).

10. W. N. Hess, H. W. Patterson, R. Wallace, and E. L. Chupp, The Cosmic Ray Neutron Energy Spectrum, Phys. Rev., 116: 445-457 (1959).

11. H. W. Patterson, W. N. Hess, B. J. Moyer, and R. Wallace, The Flux and Spectrum of Cosmic-Ray-Produced Neutrons as a Function of Altitude, Health Phys. 2[1]: 69-72 (1959).

12. J. Baarli, CERN, private communication, March 1965.

13. C. Distenfeld, Brookhaven National Laboratory, private communication, June 1965.

14. R. Sanna, K. O'Brien, M. Alberg, S. Rothenberg, and J. McLaughlin, Nuclear Emulsion Spectrometry at Low and Intermediate Neutron Energies, HASL-162, July 1965.

15. J. B. McCaslin, Some Uses and Characteristics of MOS Transistors for Health Physics Applications, USAEC Report UCRL-16446, Lawrence Radiation Laboratory, July 1965; also, Proceedings of this Conference.

16. J. B. McCaslin, A High Energy Neutron Dosimeter, Health Phys. 2: 399-407 (1960).

17. W. N. Hess, H. W. Patterson, and R. Wallace, Delay-Line Chamber Has Large Area, Low Capacitance, Nucleonics, 15[3]: 74-79 (1957).

18. E. Bruninx, High-Energy Nuclear Reaction Cross-Sections, CERN Reports CERN 61-1, January 16, 1961; CERN 62-9, February 15, 1962; CERN 64-17, March 18, 1964.

19. J. B. Cummings, Monitor Reactions for High Energy Proton Beams, Ann. Rev. Nucl. Sci., 13, 261-286 (1963).

20. H. G. De Carvalho, G. Cortini, M. Muchnik, G. G. Potenza, R. Rinzivillo, and W. O. Lock, Fission of Uranium, Thorium, and Bismuth by 20 GeV Protons, Nuovo Cimento, 27[2]: 468-475 (1963).

21. Protection Against Neutron Radiation Up to 30 Million Electron Volts, National Bureau of Standards Handbook 63, 1957.

22. Recommendations of the International Commission on Radiological Protection, I. C. R. P. Pub 4, Report of Committee IV (1953-59) on Protection against Electromagnetic Radiation above 3 MeV and Electrons, Neutrons, and Protons; (adopted 1962; with revisions adopted 1963), Pergamon Press, Oxford (1964).

23. R. H. Thomas, The Radiation Field Observed Around High-Energy Nuclear Accelerators, in Proceedings of 11th International Congress of Radiology, Rome, September 1965.

24. C. D. Zerby and W. E. Kinney, Calculated Tissue Current-to-Dose Conversion Factors for Nucleons Below 400 MeV, Nucl. Instr. Methods, 36: 125-140 (1965).

25. H. A. Dakin, Lawrence Radiation Laboratory, private communication, July 1965.

26. B. J. Moyer, Evaluation of Shielding Required for the Improved Bevatron; in Proceedings of the Conference on Shielding Near Large Accelerators, Saclay, France, 1962, Presses Universitaires de France, Paris.

27. H. W. Patterson, The Effect of Shielding on Radiation Produced by the 730-MeV Synchrocyclotron and the 6.3-GeV Proton Synchrotron at the Lawrence Radiation Laboratory, in Proceedings of the Conference on Shielding Near Large Accelerators, Saclay, France, January 1962, Presses Universitaires de France, France.

28. R. G. Alsmiller, Jr., and J. E. Murphy, Nucleon-Meson Cascade Calculations: The Star Density Produced by a 24-GeV Proton Beam in Heavy Concrete, USAEC Report ORNL-3367, Oak Ridge National Laboratory.

29. R. J. Riddell, High Energy Nuclear Cascades in Matter, USAEC Report UCRL-11989, Lawrence Radiation Laboratory, April 1965.

FIGURE CAPTIONS

Fig. 1. Gamma-ray spectra from aluminum disc: shield array experiment at Bevatron.

Fig. 2. Gamma-ray spectra from titanium disc: shield array experiment at Bevatron.

Fig. 3. Plan view of shield array.

Fig. 4. Working face of shield array.

Fig. 5. Detectors positioned in wooden troughs.

Fig. 6. Excitation function for $Ni^{58}(n, p)Co^{58}$.

Fig. 7. Excitation function for $Fe^{56}(n, p)Mn^{56}$.

Fig. 8. Excitation function for $Al^{27}(n, \alpha)Na^{24}$.

Fig. 9. Excitation function for $Mg^{24}(n, p)Na^{24}$.

Fig. 10. Excitation function for $Co^{59}(n, 2n)Co^{58}$.

Fig. 11. Excitation function for $I^{127}(n, 2n)I^{126}$.

Fig. 12. Excitation function for $Ti^{48}(n, p)Sc^{48}$.

Fig. 13. Measured neutron-energy spectra in the shield array at locations 4'-1' and 4'-3'; step-function method used for calculation.

Fig. 14. Measured neutron-energy spectra in the shield array at locations 8'-2' and 8'-4'; step-function method used for calculation.

Fig. 15. Gamma-ray peaks from several scandium isotopes produced in titanium: hypothetical structure showing resolution capability of Ge(Li) detector.

Fig. 16. Gamma-ray spectra from 8-in.-diam by 1-in.-thick aluminum disc, showing Na^{24} shape and BKG shape.

Fig. 17. Spectral shapes observed in 5-in.-diam by 5-in.-thick plastic scintillator, showing C^{11} and BKG shapes.

Fig. 18. Bismuth fission counter response, showing integral bias curves from actual Bevatron data and internal Cf^{252} check source.

Table 1. Threshold detectors.

Reaction	Theoretical[a] threshold (MeV)	Effective[a] threshold (MeV)	Half life of residual nucleus	Form of detector
$Ni^{58}(n, p)Co^{58}$	-0.4	1.2	71 days	4-in. metal disc
$Al^{27}(n, p)Mg^{27}$	1.8	2.7	9.5 min	4-in. metal disc
$Co^{59}(n, \alpha)Mn^{56}$	-0.3	5.3	2.58 h	4-in. metal disc
$Fe^{56}(n, p)Mn^{56}$	2.9	5.0	2.58 h	4-in. metal disc
$Ti^{48}(n, p)Sc^{48}$	3.2	5.2	44.0 h	4-in. metal disc
$Mg^{24}(n, p)Na^{24}$	4.7	6.1	15.0 h	4-in. metal disc
$Al^{27}(n, \alpha)Na^{24}$	3.1	5.9	15.0 h	4-in. metal disc
$I^{127}(n, 2n)I^{126}$	9.3	9.4	13.2 days	Boxed crystals
$Co^{59}(n, 2n)Co^{58}$	10.2	10.8	71 days	4-in. metal disc
$Ni^{58}(n, 2n)Ni^{57}$	11.8	12.5	36 h	4-in. metal disc

[a]The theorectical threshold is calculated as $-Q \times \frac{1+M}{M}$, where Q is the Q value for the reaction and M is the mass number of the target nucleus. The effective threshold is the energy at which the cross section is 1/100 of its peak value.

Table 2. Additional threshold reactions

Reactions	Theorectical threshold (MeV)	Half life of residual nucleus
$Zn^{64}(n, p)Cu^{64}$	-0.2	12.9 hr
$Co^{59}(n, p)Fe^{59}$	0.8	45 days
$Cr^{52}(n, p)V^{52}$	3.1	3.77 min
$Mn^{55}(n, \alpha)V^{52}$	0.6	3.77 min
$V^{51}(n, \alpha)Sc^{48}$	1.6	44.0 h
$Tl^{203}(n, 2n)Tl^{202}$	8.8	12.0 days
$Sb^{121}(n, 2n)Sb^{120g}$	9.3	16 min
$Cu^{63}(n, 2n)Cu^{62}$	10.6	9.9 min
$Cu^{65}(n, 2n)Cu^{64}$	10.1	12.9 h
$Sc^{45}(n, 2n)Sc^{44m}$	11.6	2.4 days
$Na^{23}(n, 2n)Na^{22}$	12.9	2.6 y
$F^{19}(n, 2n)F^{18}$	11.0	1.87 h
$Zn^{64}(n, 2n)Zn^{63}$	11.8	38 min
$Fe^{54}(n, 2n)Fe^{53}$	13.6	9.0 min
$P^{31}(n, 2n)P^{30}$	12.7	2.55 min
$In^{115}(n, 2n)In^{114m}$	9.1	50.0 days
$As^{75}(n, 2n)As^{74}$	10.4	18 days
$Au^{197}(n, 2n)Au^{196g}$	8.1	6.1 days
$C^{12}(n, 2n)C^{11}$	20.3	20.4 min
$Si^{28}(n, p)Al^{28}$	3.99	2.3 min
$Cu^{65}(n, p)Ni^{65}$	1.3	2.65 h
$In^{115}(n, n')In^{115m}$	0.2	4.6 h
$Rh^{103}(n, n')Rh^{103m}$	0.04	54 min
$P^{31}(n, \alpha)Al^{28}$	2.0	2.3 min
$Mo^{92}(n, 2n)Mo^{91}$	13.3	16 min

Table 3. Step-function solution values for Bevatron shield neutron spectra.

Energy interval (MeV)	$\phi(E)$			
	Fig. 13 $4'-1'$	Fig. 13 $4'-3'$	Fig. 14 $8'-2'$	Fig. 14 $8'-4'$
2-6	2.38×10^6	2.78×10^5	3.0×10^5	5.9×10^4
6-11	0.57×10^5	0.65×10^5	0.65×10^5	1.25×10^4
11-16	0.50×10^6	0.37×10^5	0.37×10^5	0.65×10^4
16-22	0.24×10^6	0.24×10^5	0.24×10^5	0.58×10^4
22-30	0.21×10^6	0.16×10^5	0.21×10^5	0.50×10^4

Table 4. Threshold reactions on natural titanium.

Reaction	Half life	γ-Energy (MeV)	Abundance	Estimated threshold (MeV)
$Ti^{48}(n, p)Sc^{48}$	44 hr	0.99 1.04 1.32	100% 100% 100%	≈5
$Ti^{47}(n, p)Sc^{47}$	3.4 d	0.16	60%	≈1.5
$Ti^{46}(n, p)Sc^{46}$	84 d	0.89 1.12	100% 100%	≈3
$Ti^{46}(n, 2n)Ti^{45}$	3.1 hr	β^+ 0.51	100% 200%	≈14
Ti ( )Sc^{44}	3.9 hr	1.16 β^+ 0.51	100% 93% 186%	
Ti ( )Sc^{44m}	2.4 d	0.27	86%	
$Ti^{48}(p, n)V^{48}$	16.1 d	0.99 1.32	100% 100%	≈7

Table 5. Detector response function values, including variation sets for aluminum, carbon, and bismuth.

Neutron energy (MeV)	Aluminum, normal (mb)	Aluminum, low (mb)	Aluminum high (mb)	Carbon, normal (mb)	Carbon, low (mb)	Carbon, medium (mb)	Carbon high (mb)	BiF normal (mb)	BiF low (mb)	BF_3, normal (relative)
0.04	0.0	0.0	0.0	0.0	0.0	0.0	0.0	0.0	0.0	0.80
0.14	0	0	0	0	0	0	0	0	0	0.80
0.40	0	0	0	0	0	0	0	0	0	1.1
1.40	0	0	0	0	0	0	0	0	0	1.2
4.0	0	0	0	0	0	0	0	0	0	1.1
14.0	100	100	100	0	0	0	0	0	0	1.0
40.0	15	7	15	22	20	25	40	1.0	50	0.20
140	10	7	15	22	20	25	30	80	130	0.04
400	10	7	15	22	20	25	25	170	130	0.01
1400	10	7	15	22	20	25	25	150	130	0.0
4000	9	7	15	22	20	25	25	150	130	0.0
Relative count rate	3.41×10^4	2.99×10^4	3.86×10^4	5.17×10^5	4.70×10^5	5.87×10^5	6.85×10^5	4.47×10^3	4.69×10^3	2.97×10^6
Percentage change	0%	-12%	+13%	0%	-9%	±14%	+32%	0%	+5%	---

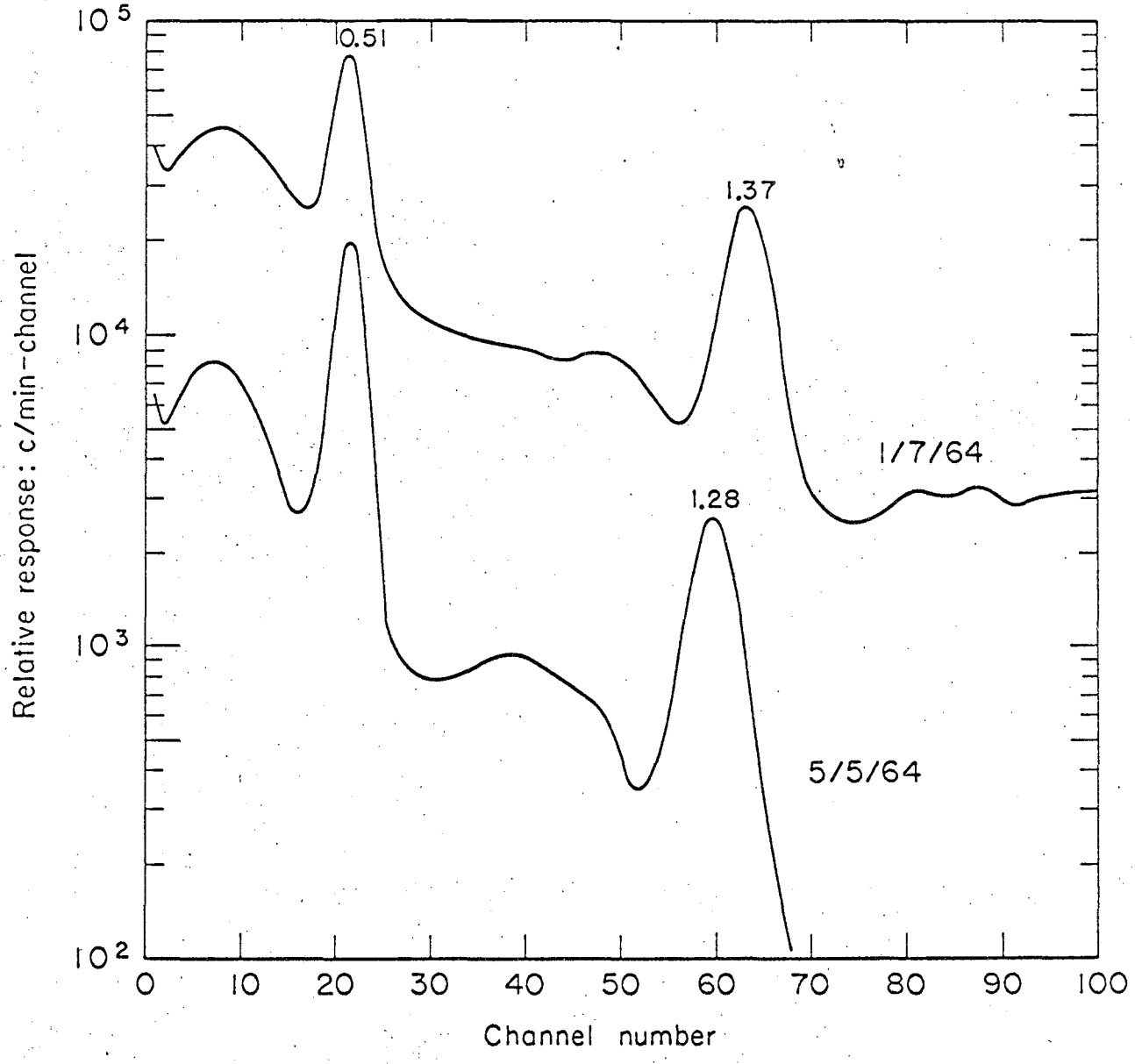

Fig. 1

MUB-8457

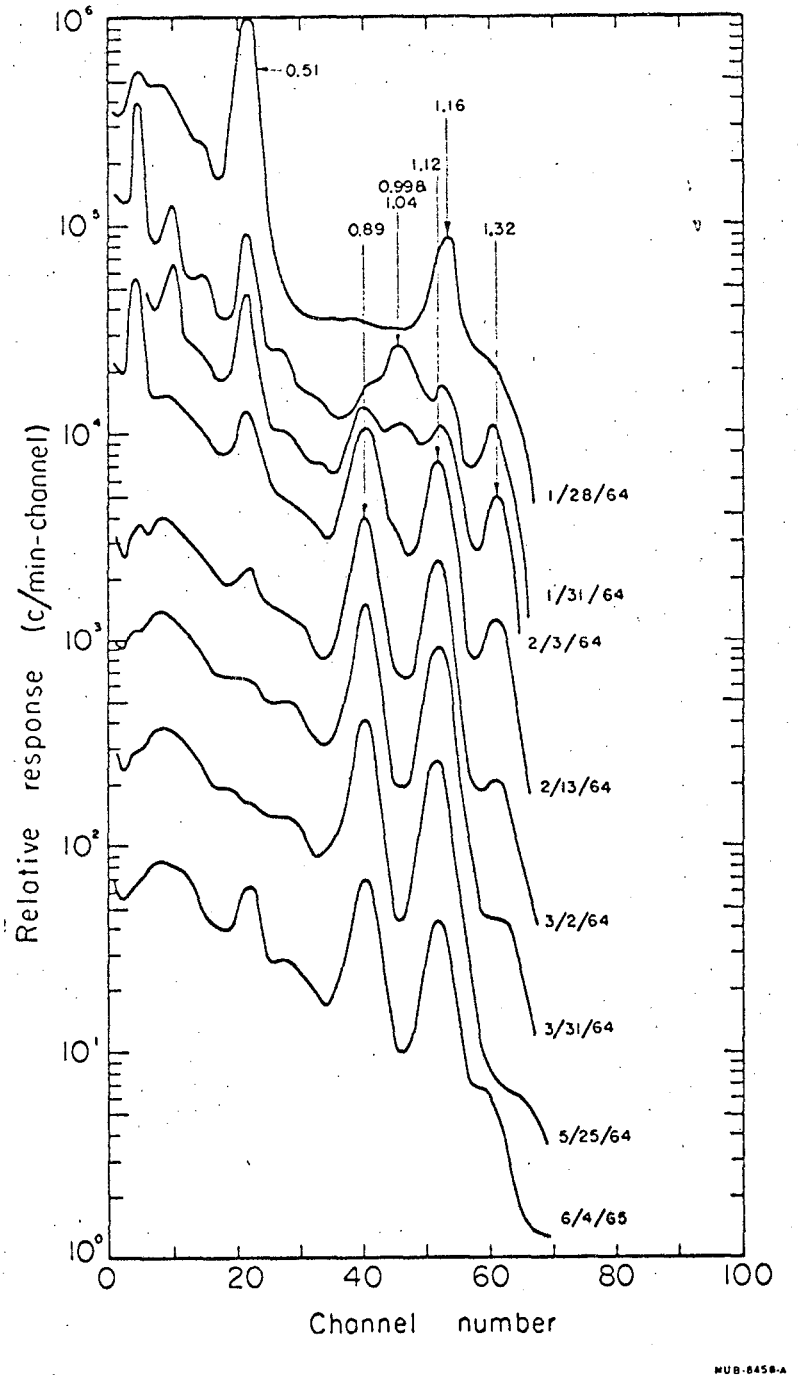
0.51
1.16
1.12
0.998
1.04
0.89
1.32
1/28/64
1/31/64
2/3/64
2/13/64
3/2/64
3/31/64
5/25/64
6/4/65
Relative response (c/min-channel)
Channel number
MUB-8458-A

Fig. 2

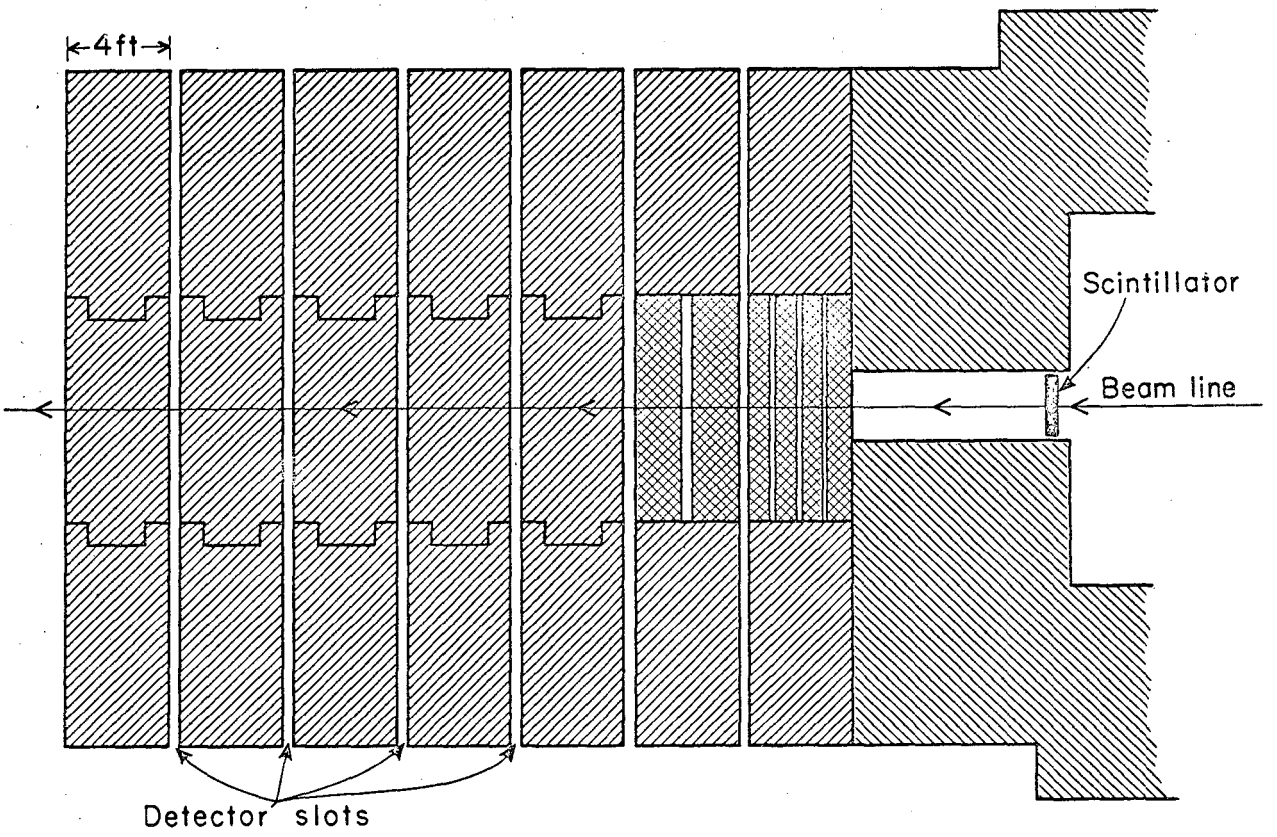

MUB-3055

Fig. 3

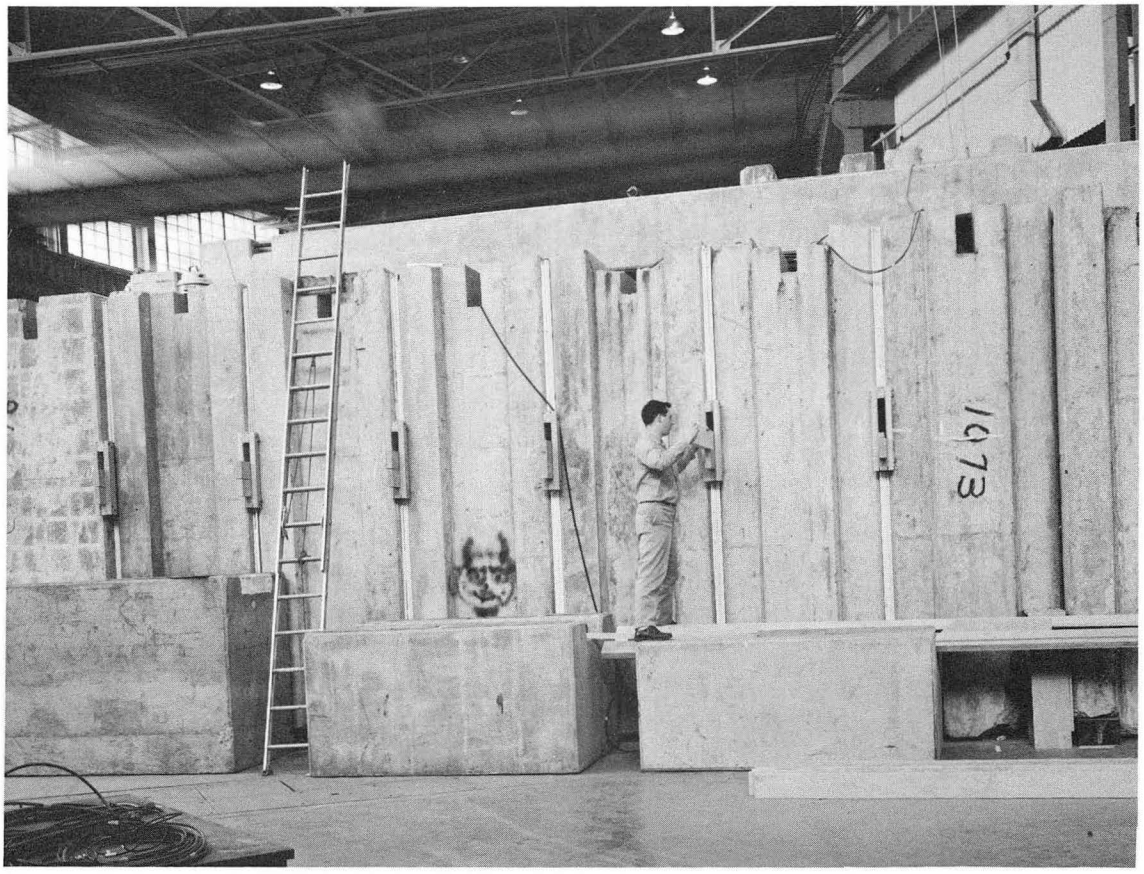

ZN-4498

Fig. 4

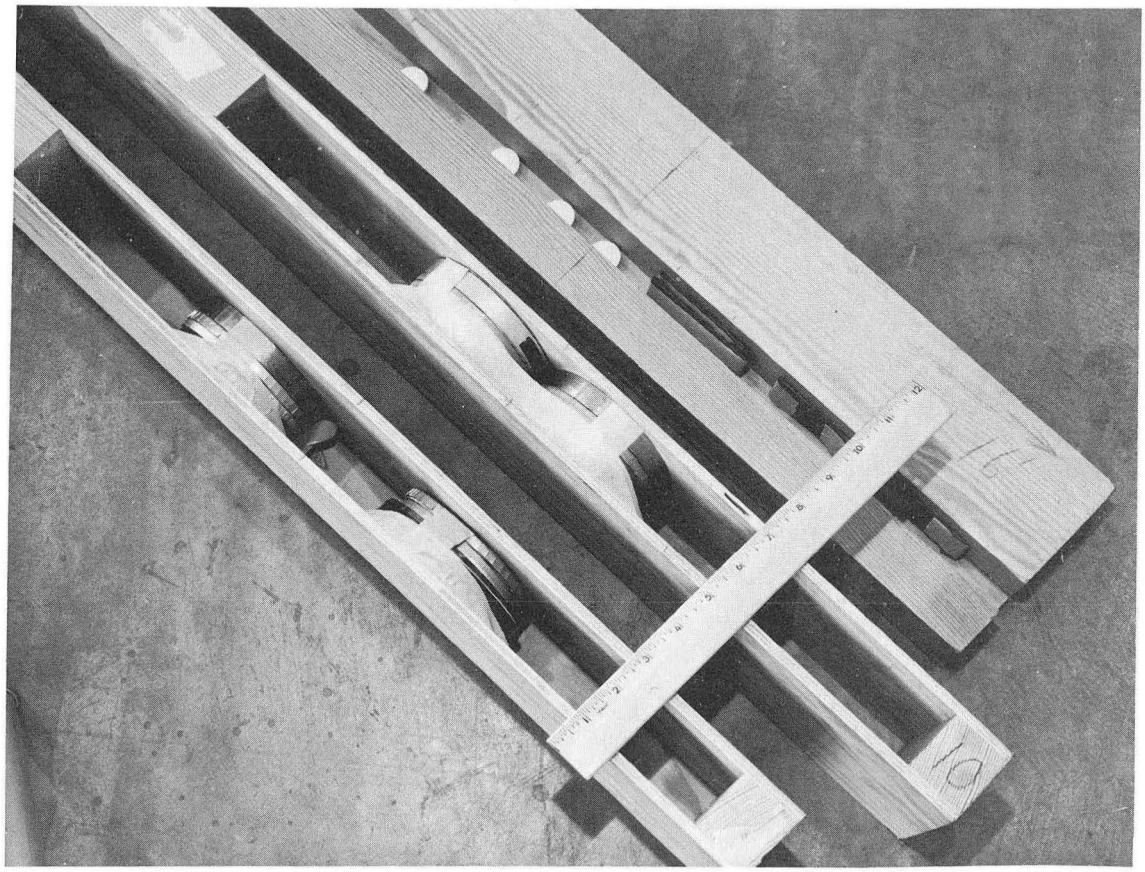

ZN-4499

Fig. 5

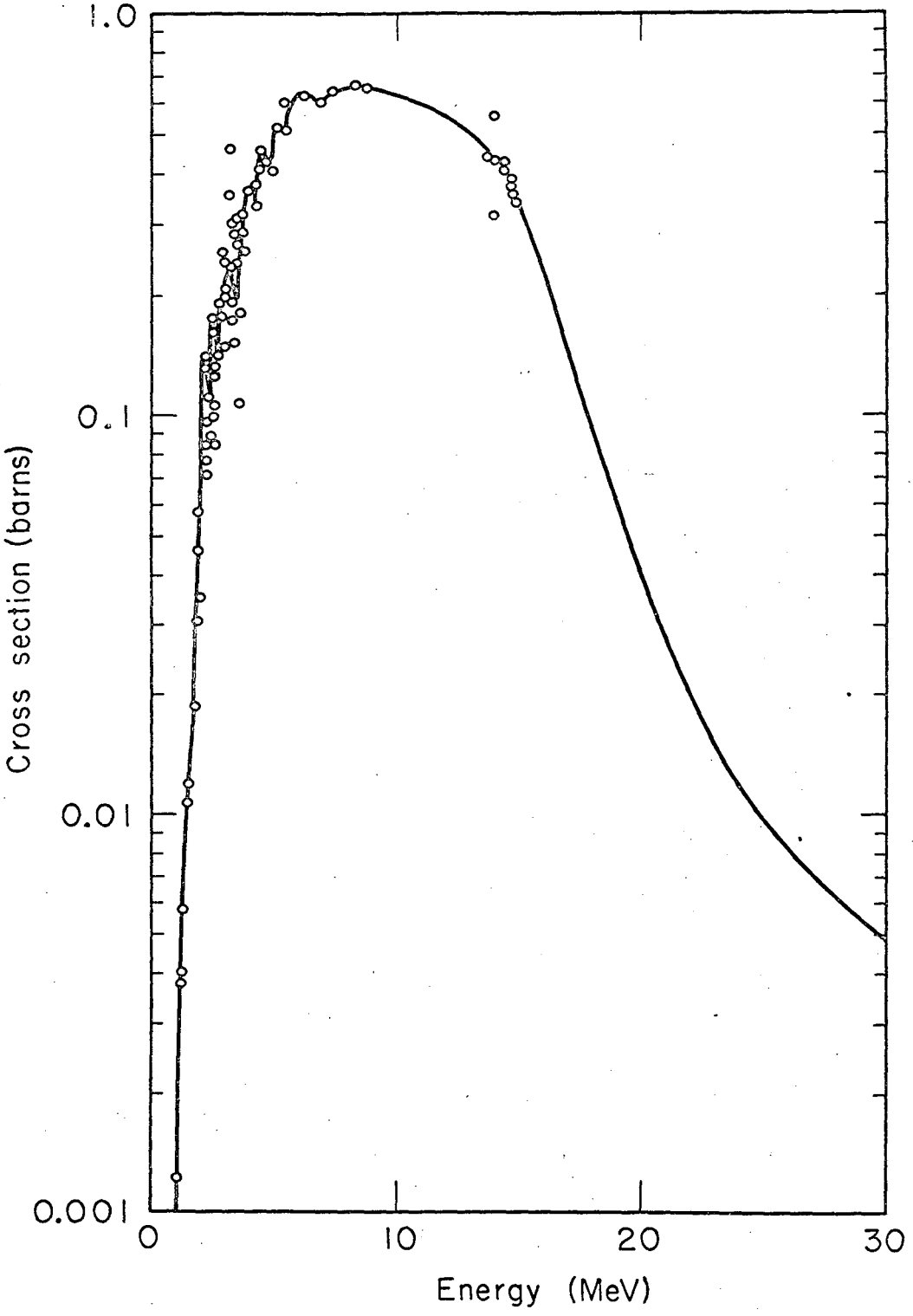

Fig. 6

MU-34976

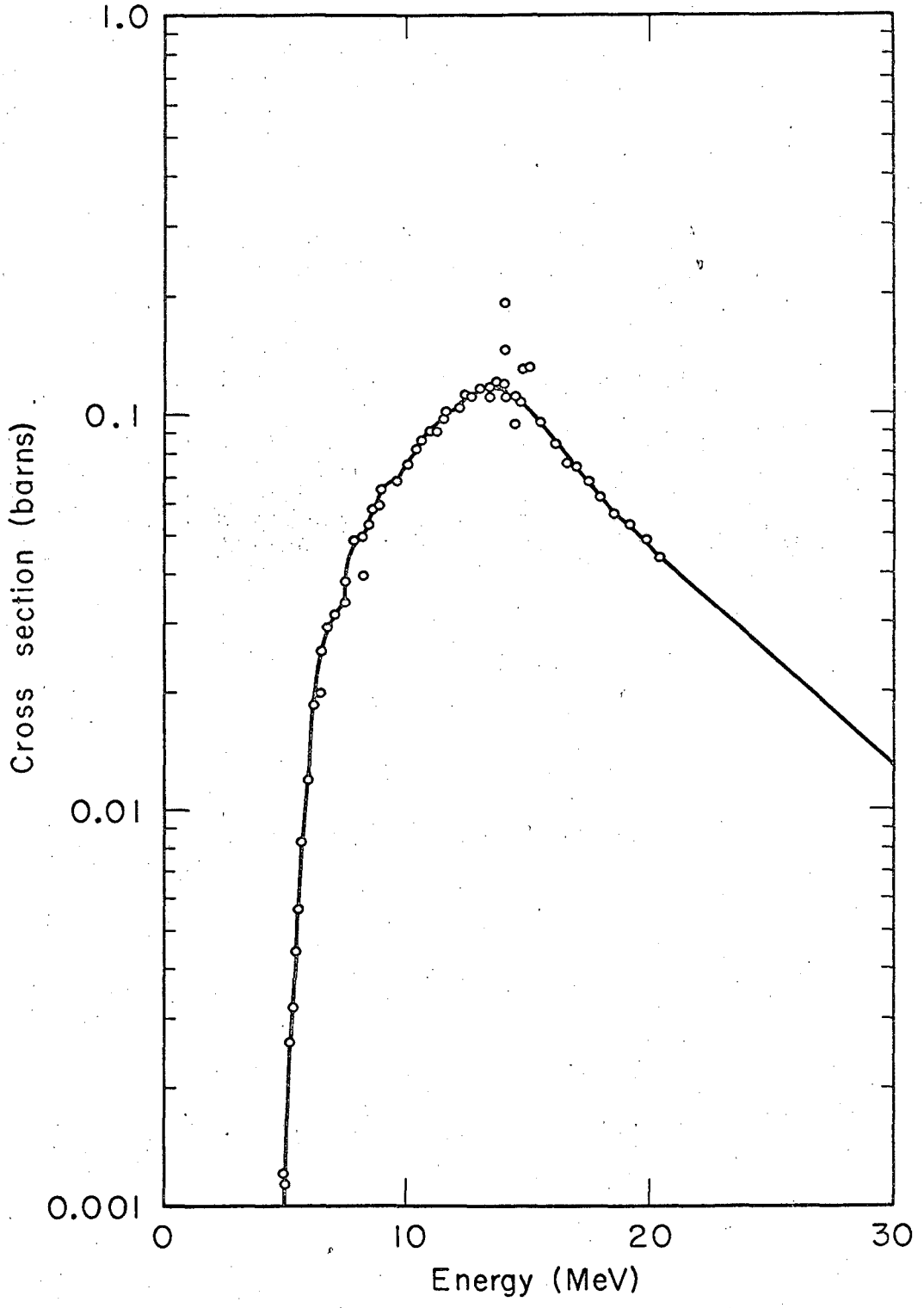

Fig. 7

MU-34979

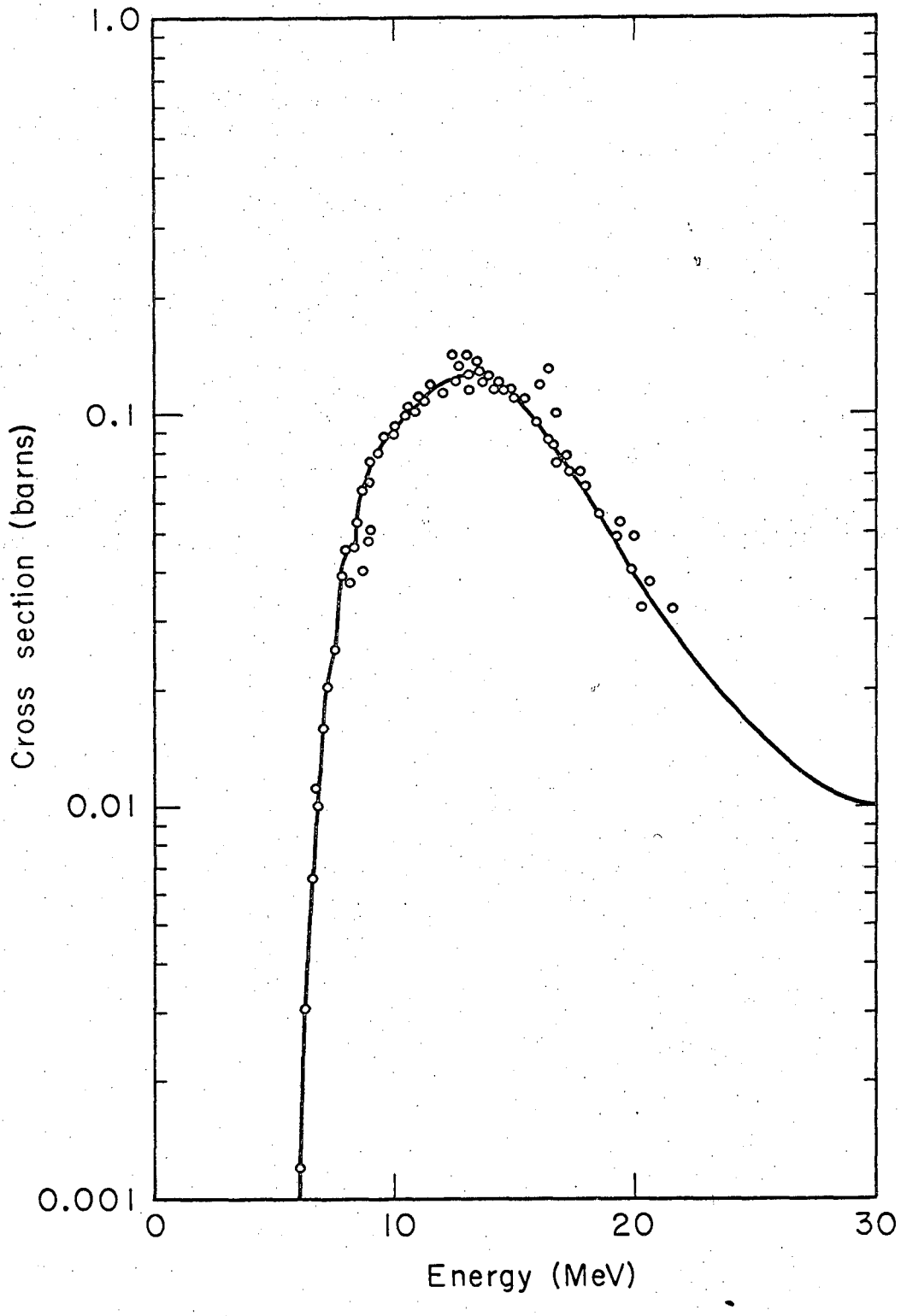

Fig. 8

MU-34982

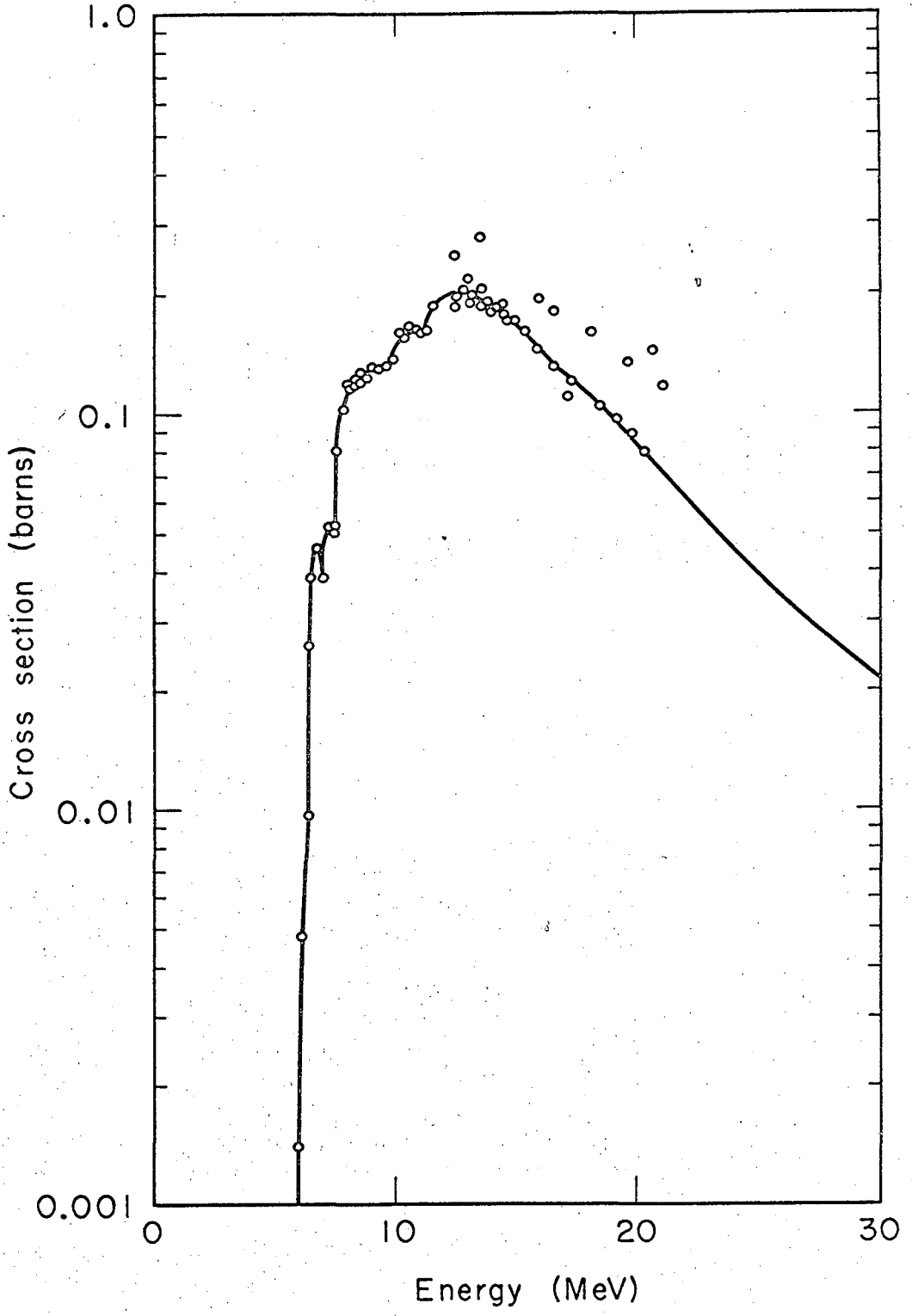

Fig. 9

MU-34981

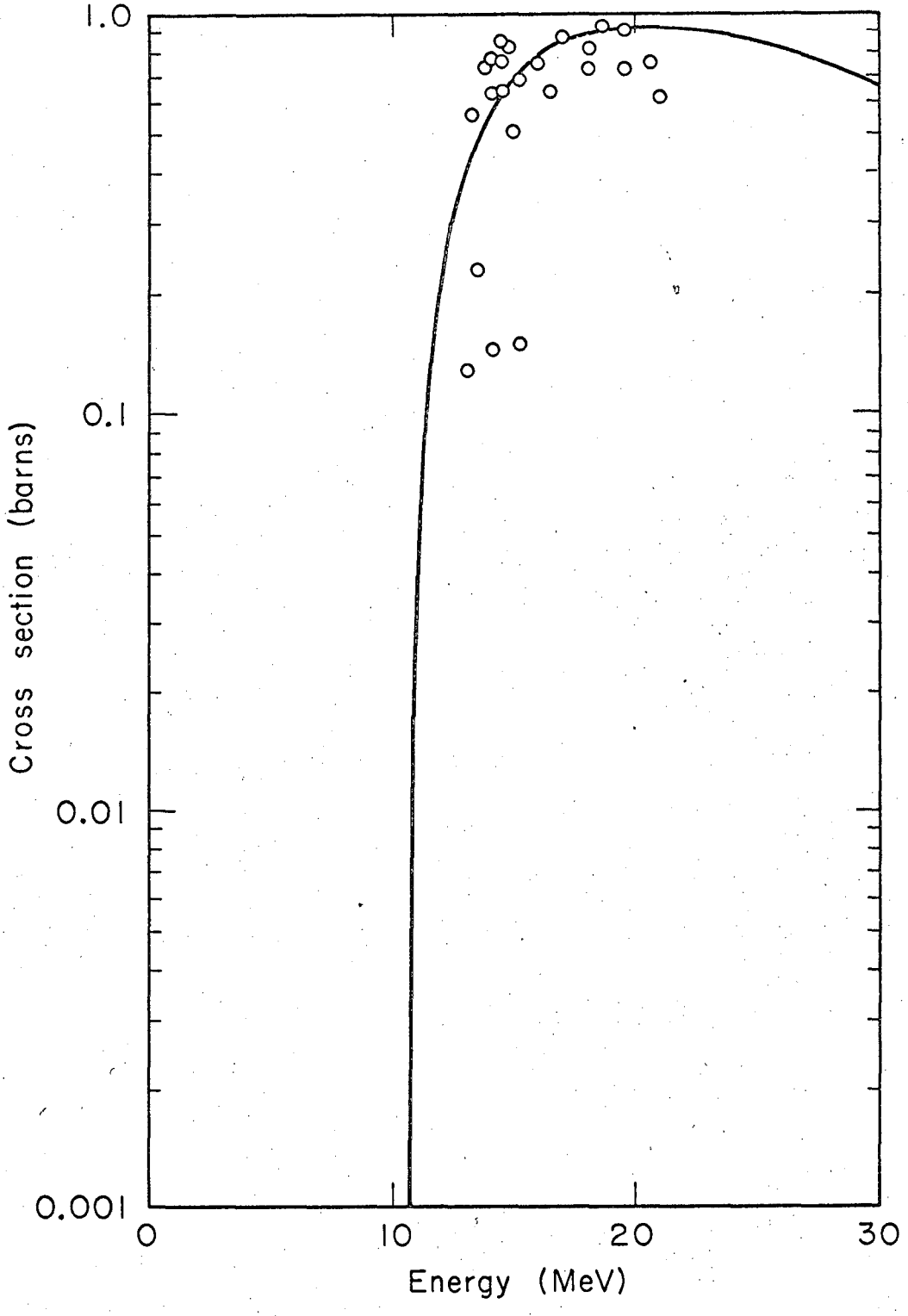

Fig. 10

MU-34984

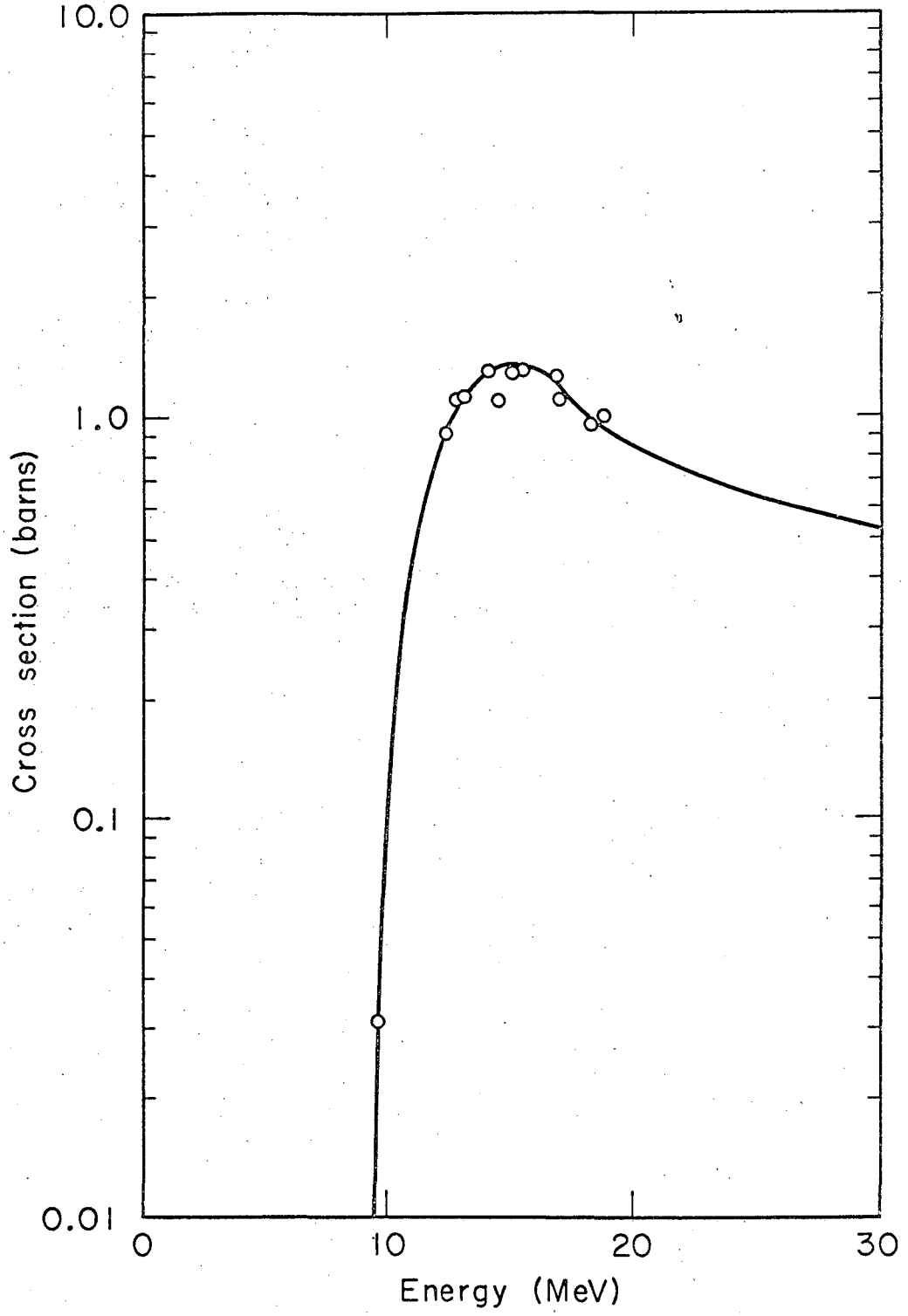

Fig. 11

MU-34983

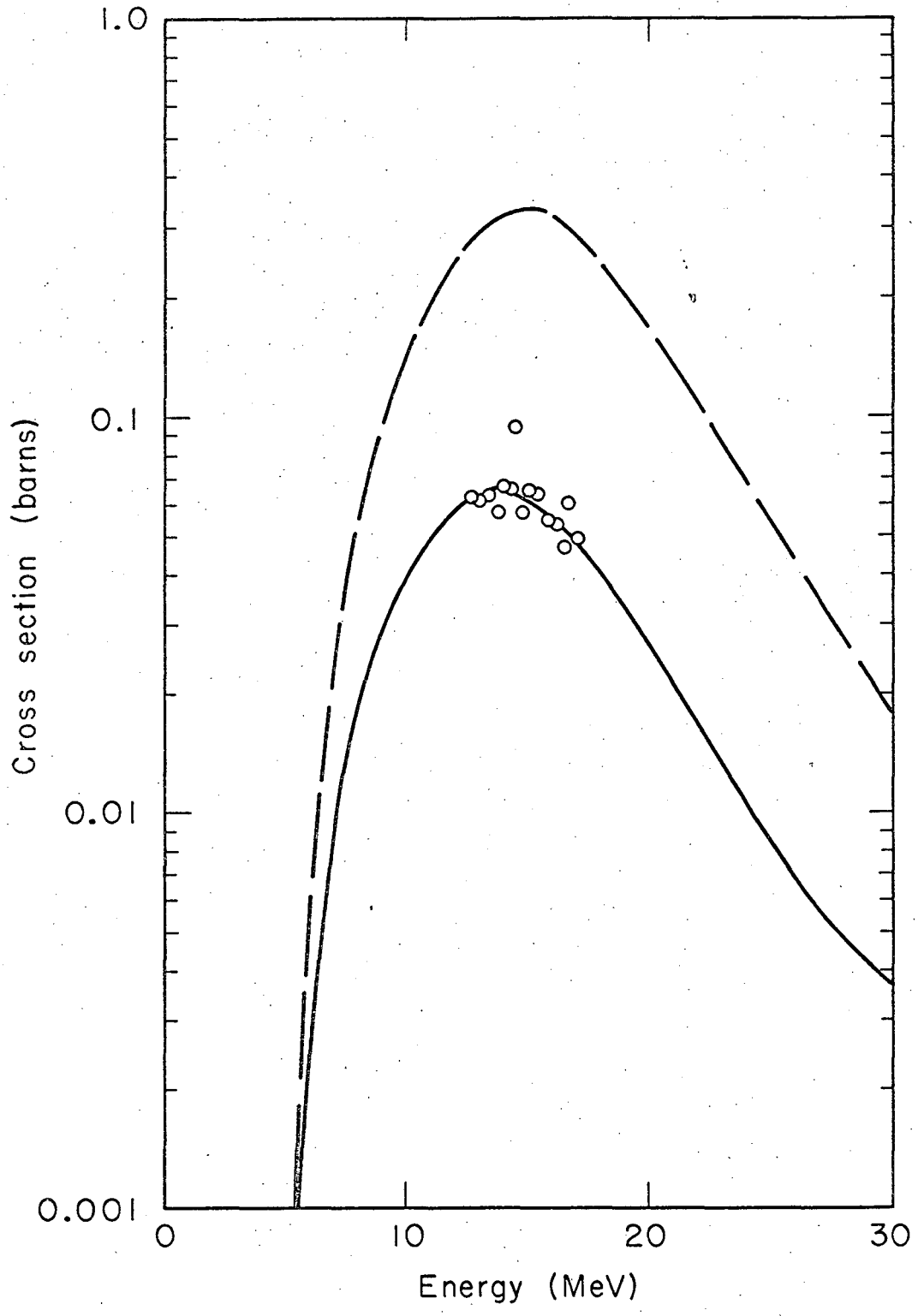

Fig. 12

MU-34980

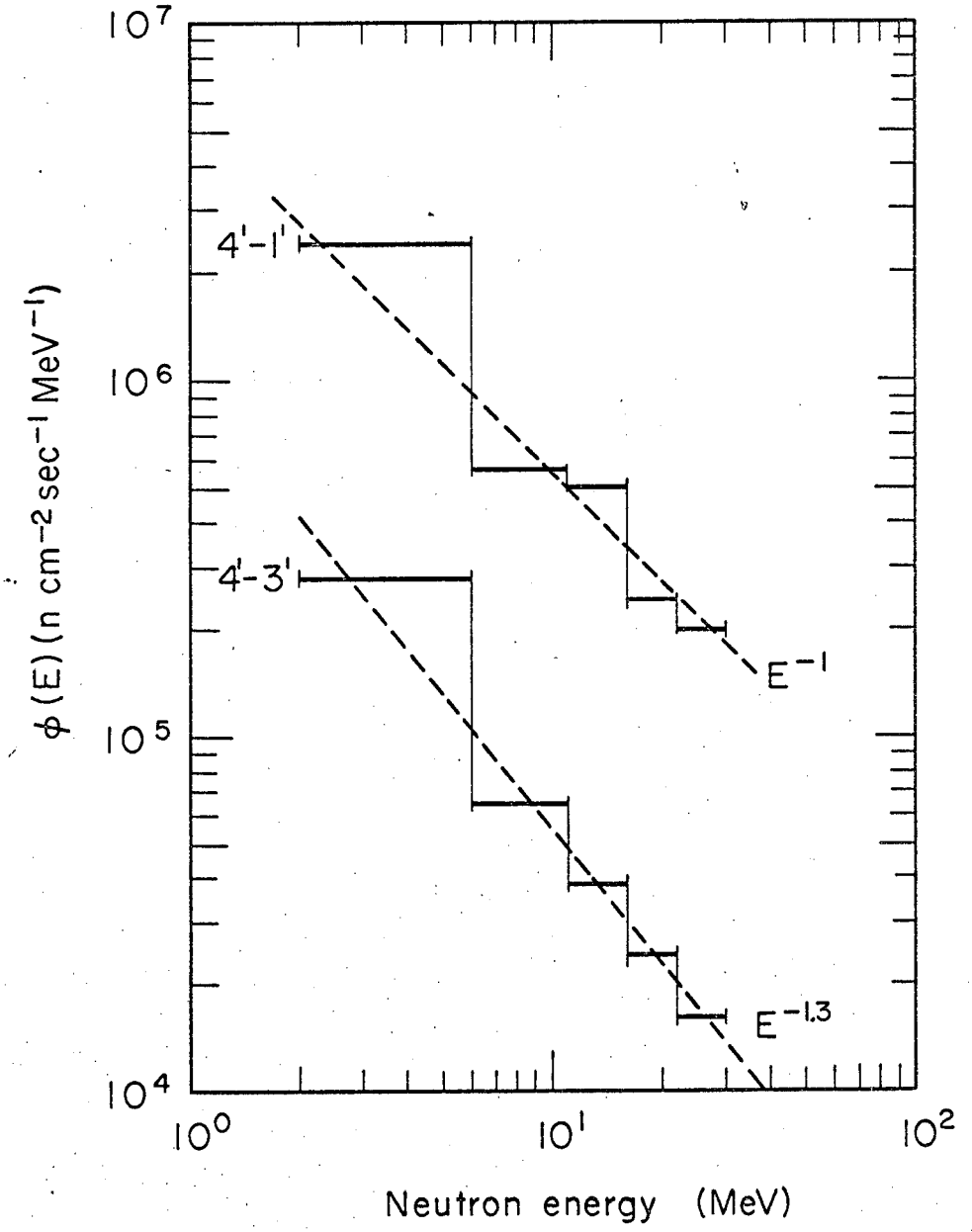

MUB-8450

Fig. 13

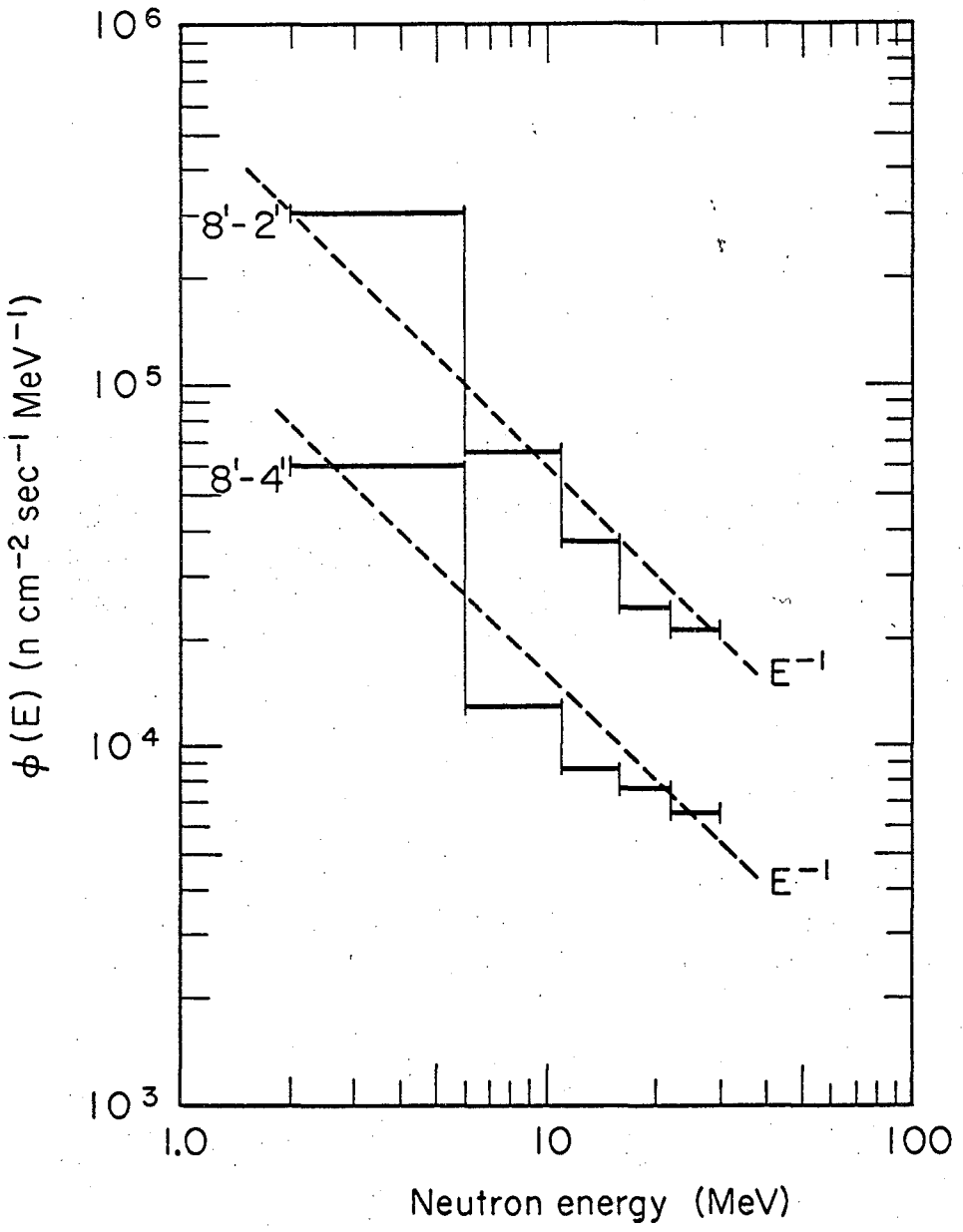

Fig. 14

MUB-8451

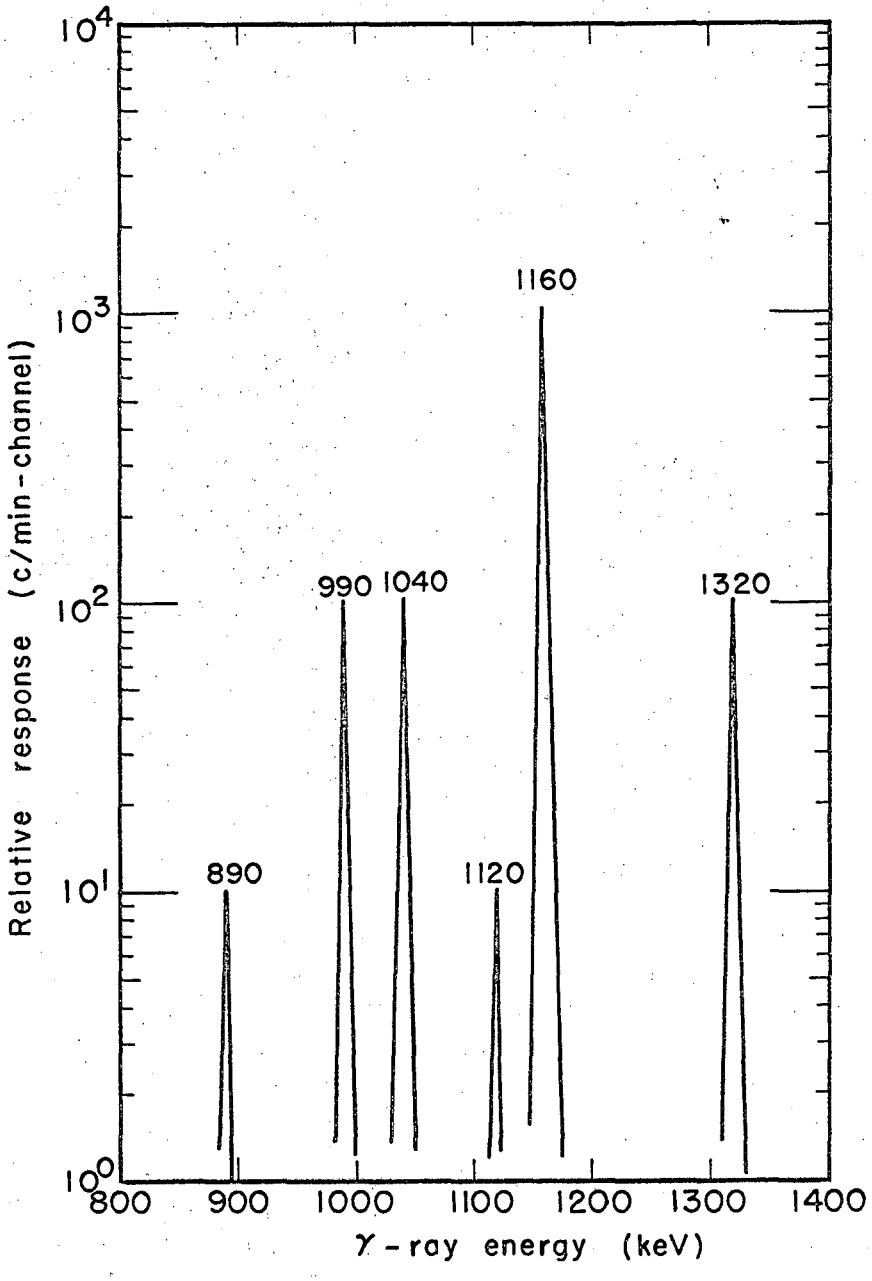

MUB-8613

Fig. 15

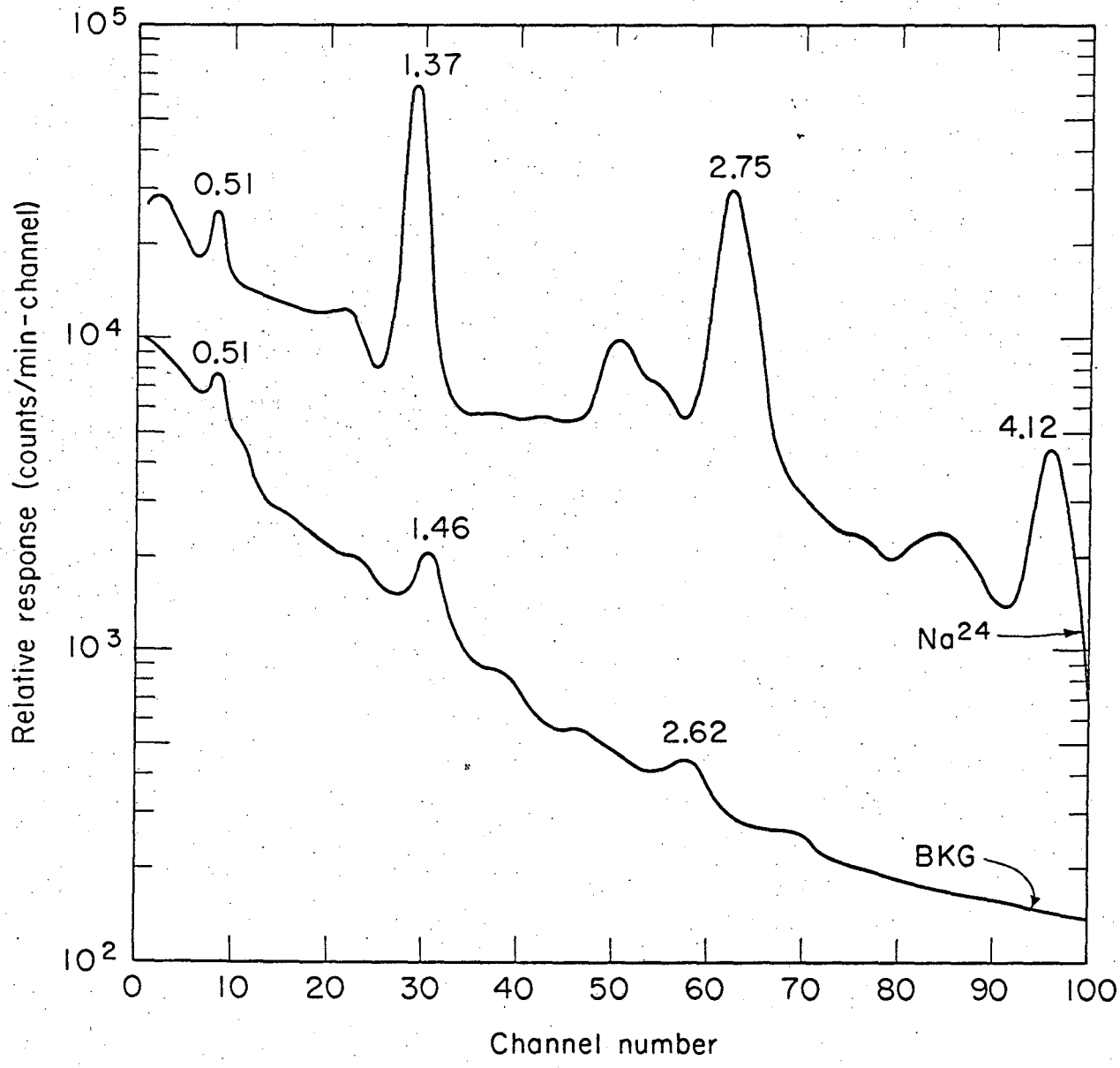

MUB-8504

Fig. 16

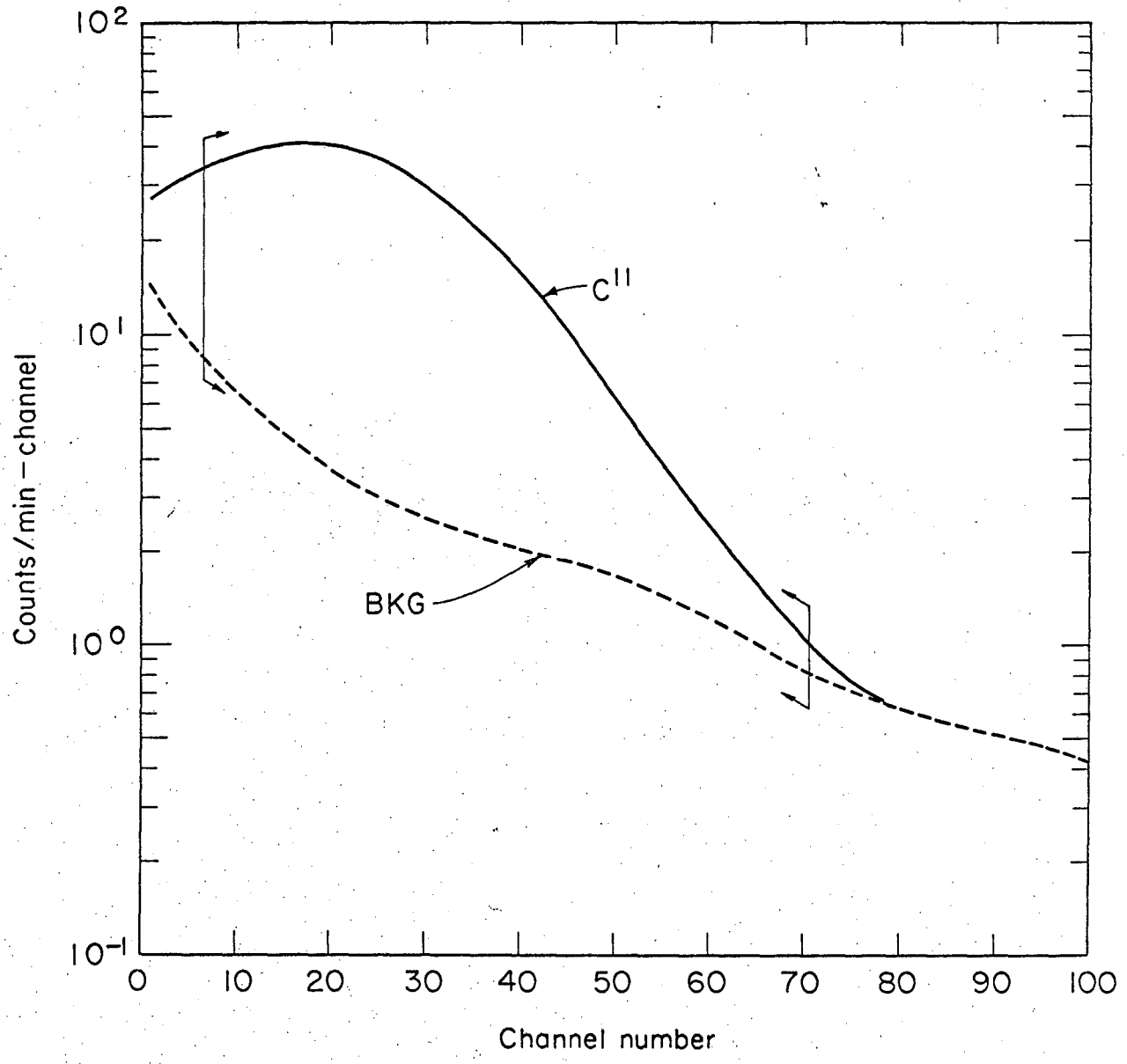

Fig. 17

MUB-8503

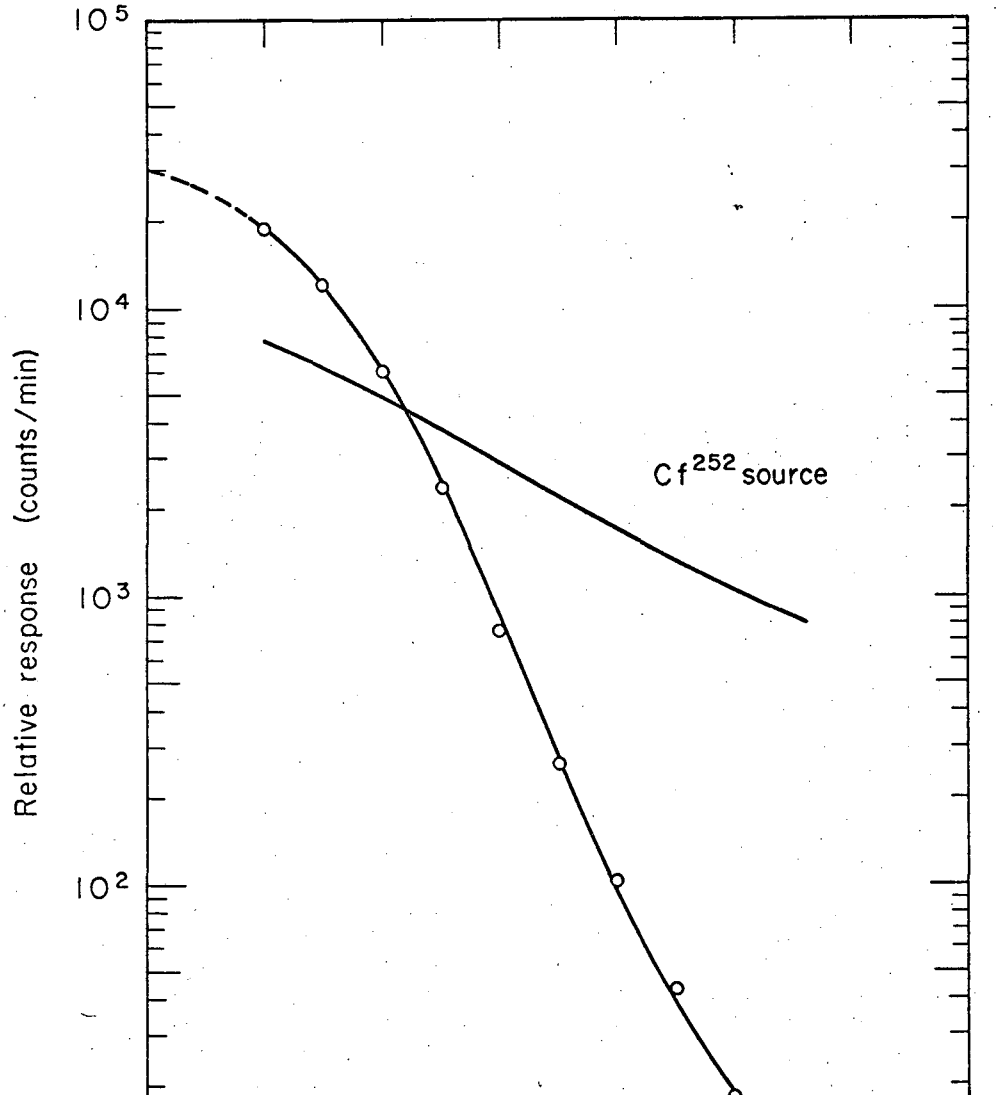

Fig. 18

MUB-8502

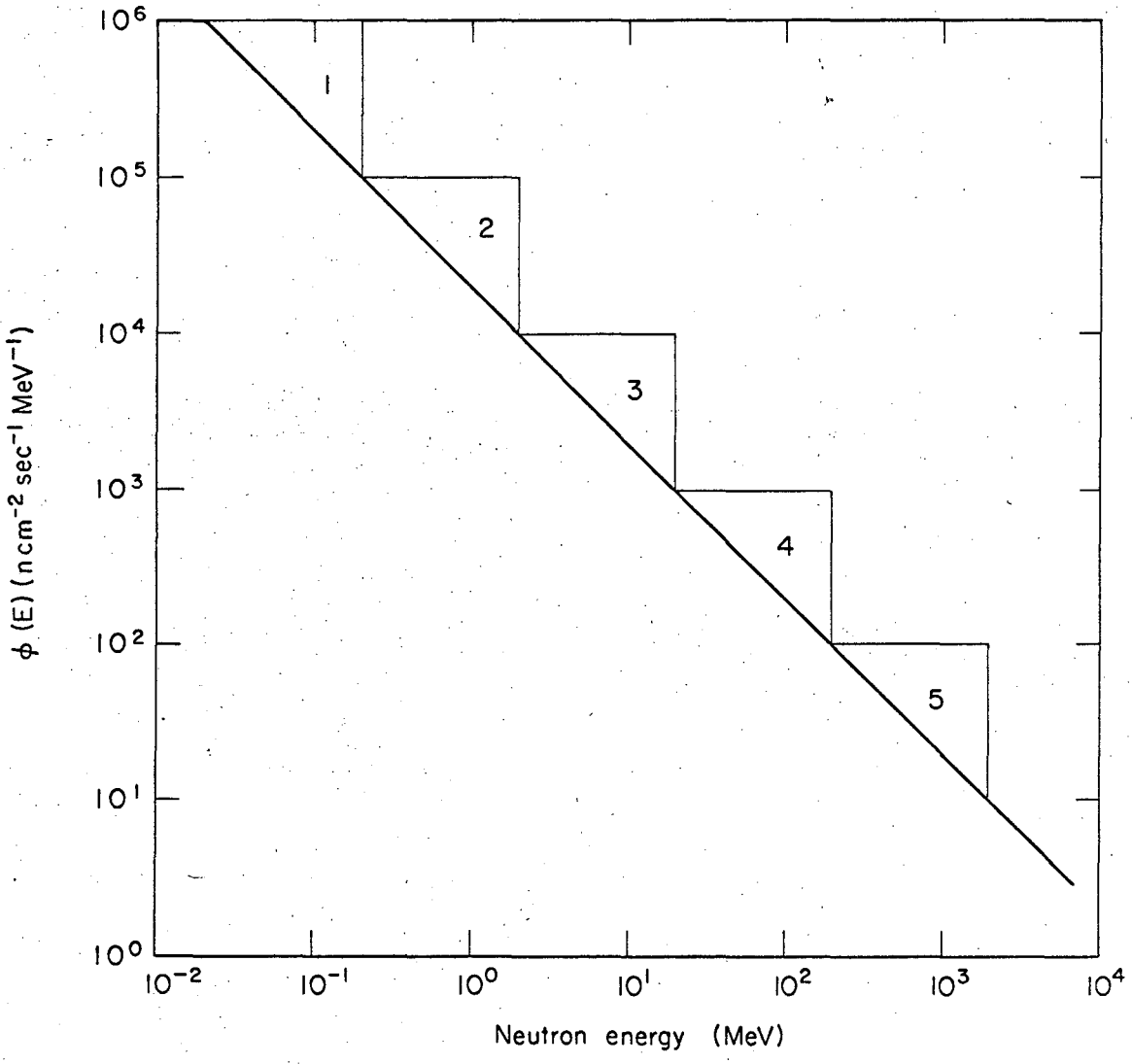

Fig. 19

MUB-8452

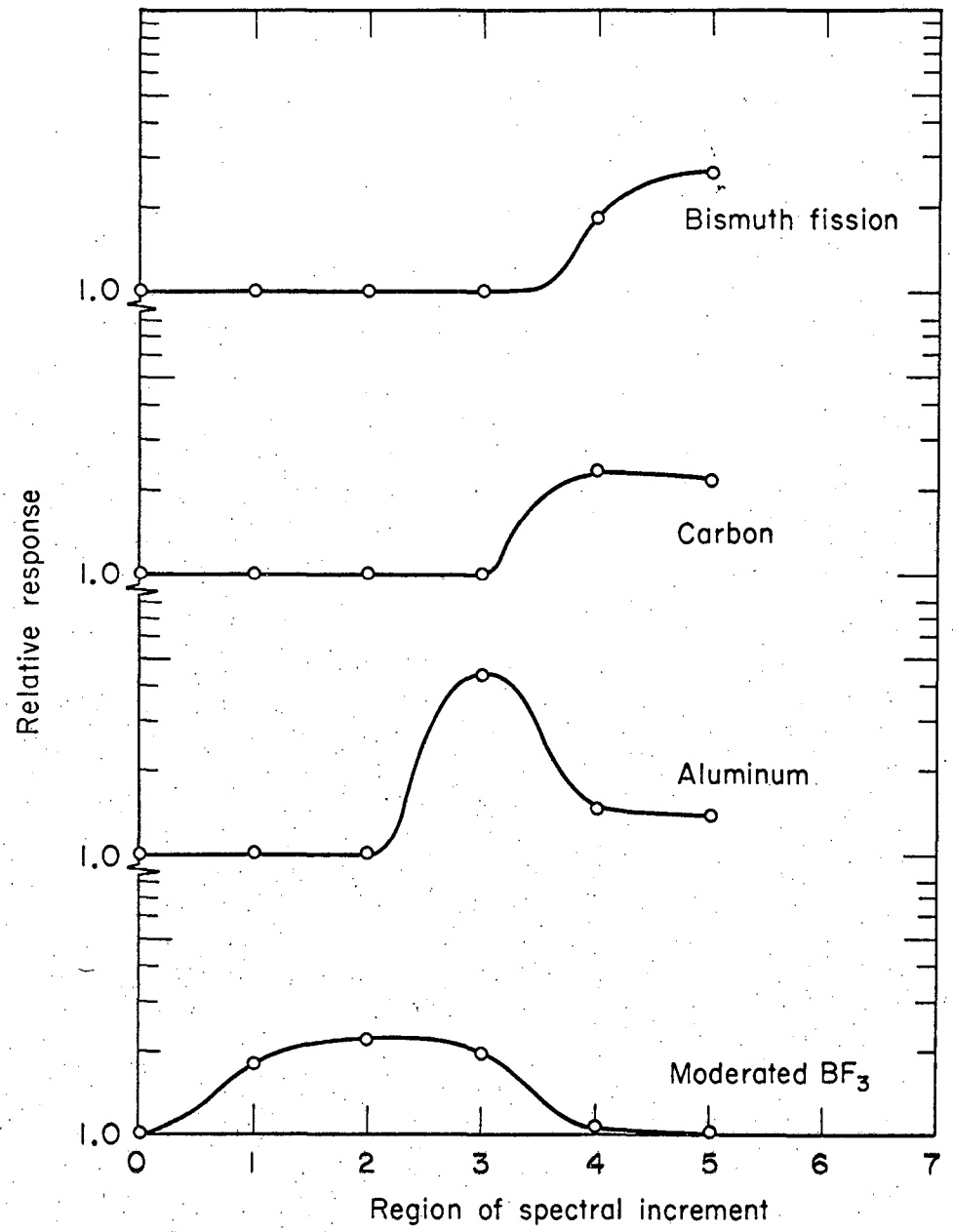

Fig. 20

MUB-8453

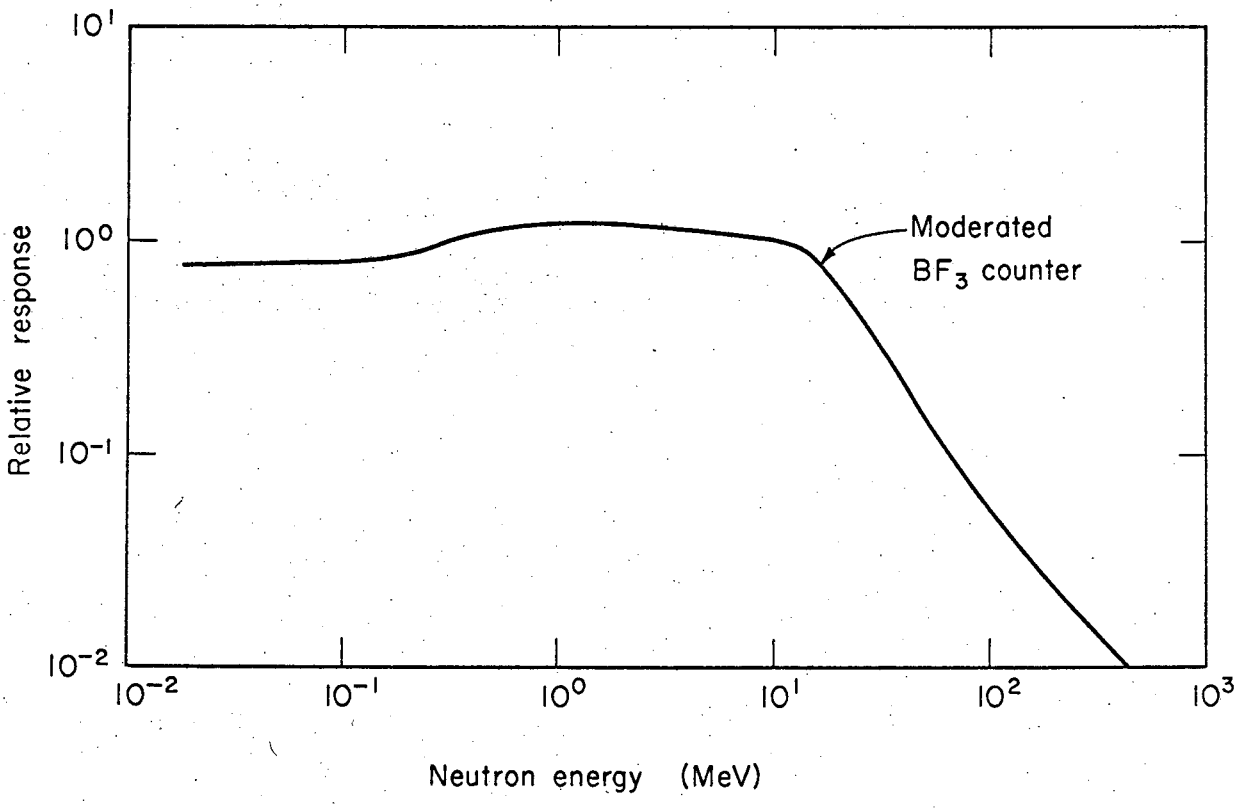

MUB-8501

Fig. 21

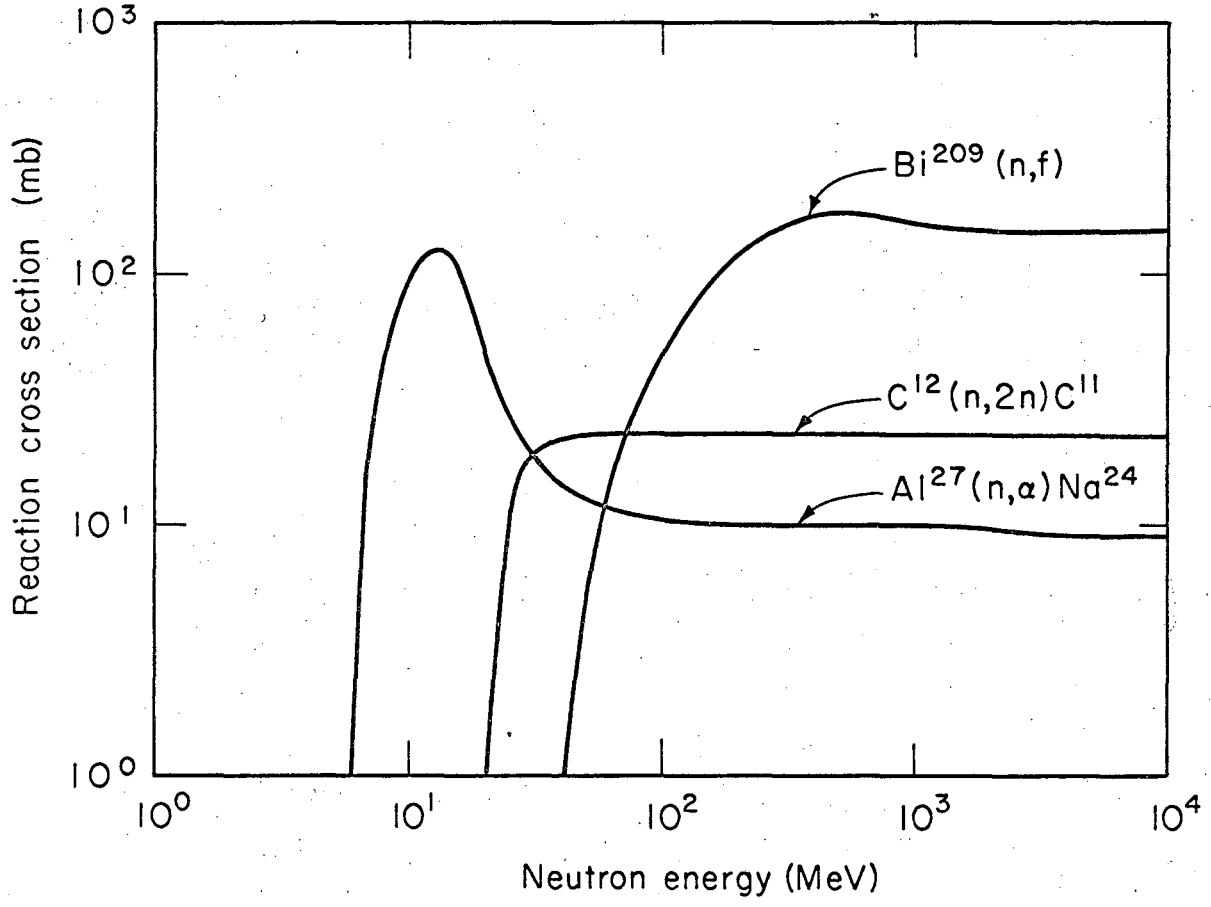

MUB-8500

Fig. 22

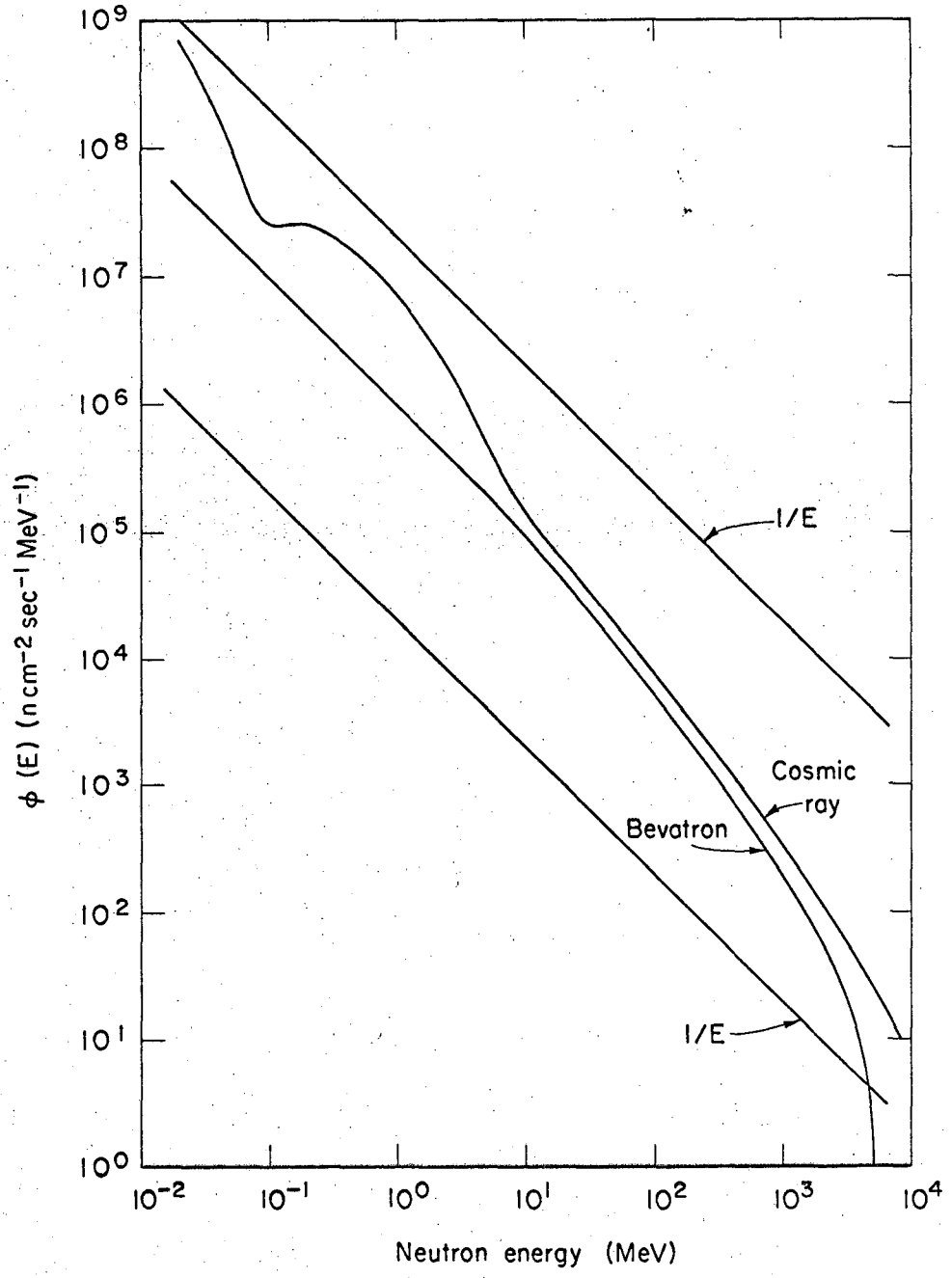

MUB-8454

Fig. 23

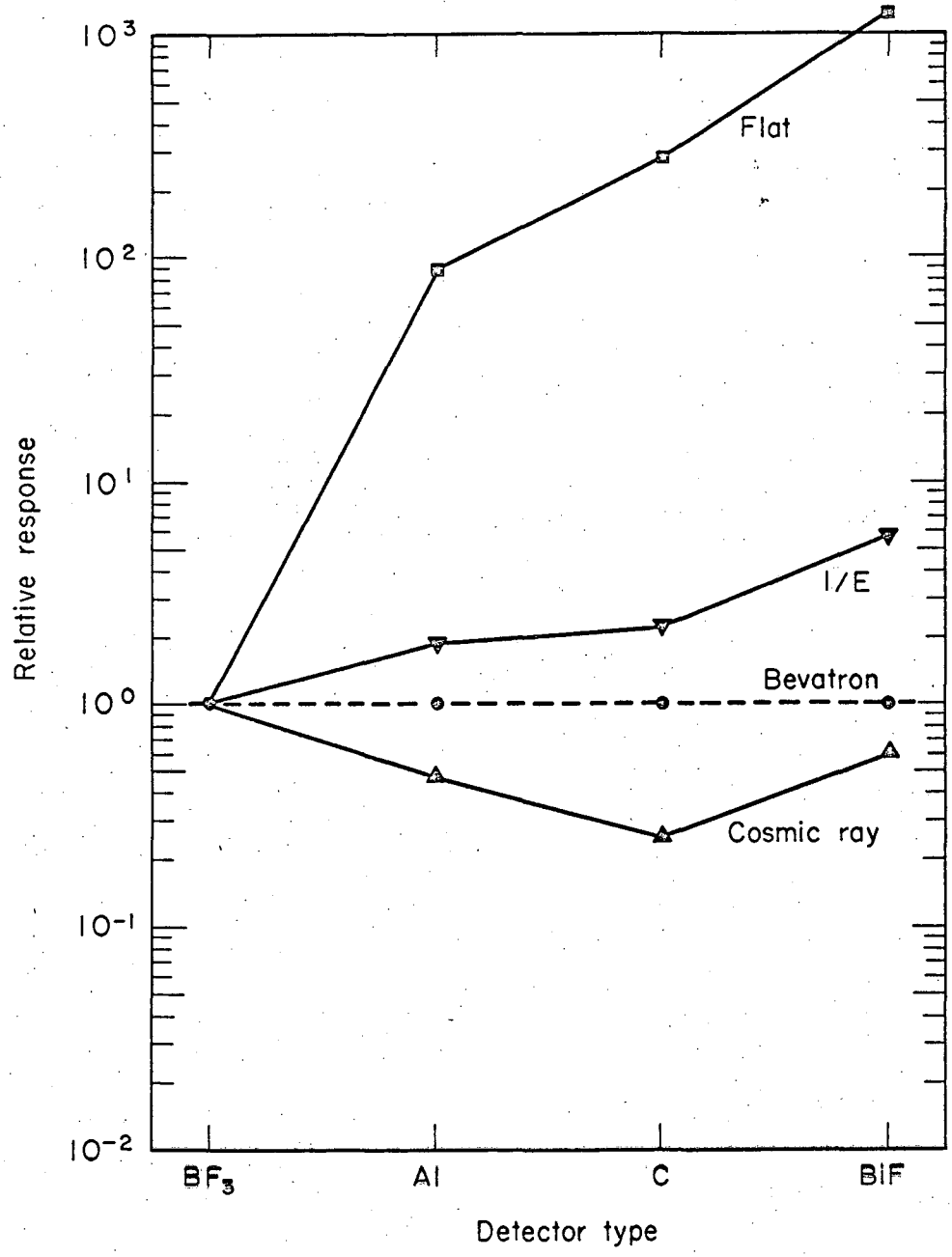

Fig. 24

MUB-8455

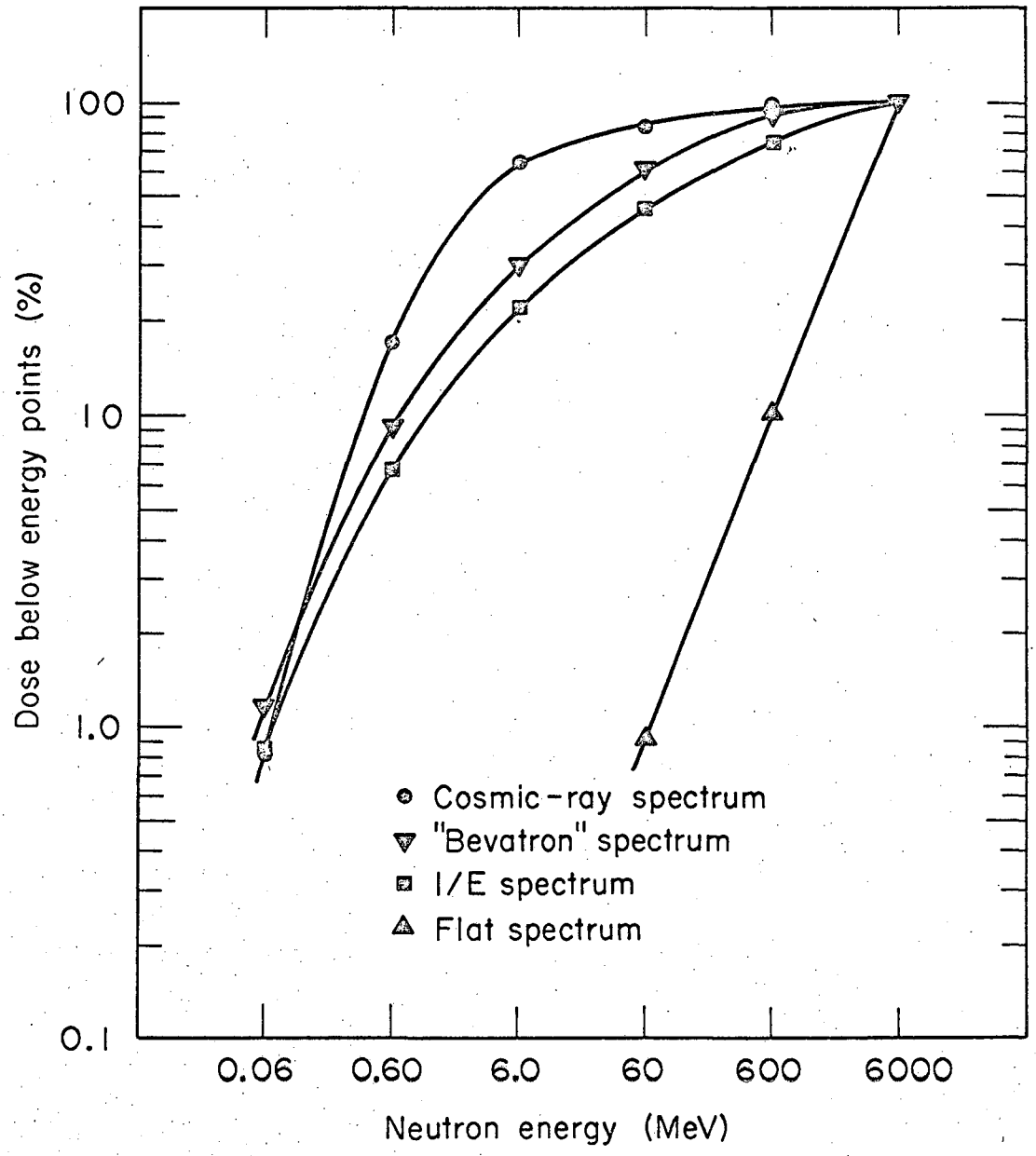

Fig. 25

MUB-8456